

1 **Dynamics of corticospinal motor control**
2 **during overground and treadmill**
3 **walking in humans**

4 Luisa Roeder^{1,2}, Tjeerd W Boonstra^{3,4}, Simon S Smith⁵, Graham K Kerr^{1,2}

5

6 ¹ Movement Neuroscience Group, Institute of Health and Biomedical Innovation, Queensland
7 University of Technology, Brisbane, Australia

8 ² School of Exercise and Nutrition Sciences, Queensland University of Technology, Brisbane,
9 Australia

10 ³ Black Dog Institute, University of New South Wales, Sydney, Australia

11 ⁴ Systems Neuroscience Group, QIMR Berghofer Medical Research Institute, Brisbane,
12 Australia

13 ⁵ Institute of Social Science Research, University of Queensland, Brisbane, Australia

14

15 **Running head:** Corticospinal dynamics during overground and treadmill gait

16 **Address for correspondence:**

17 Luisa Roeder, Ph.D.

18 Institute of Health and Biomedical Innovation

19 School of Exercise and Nutrition Sciences

20 Queensland University of Technology

21 60 Musk Ave, Kelvin Grove, Queensland 4059, AUSTRALIA

22 Tel: +61 73138 6428; Fax: +61 73138 6030

23 Email: l.roeder@qut.edu.au

24 **Abstract**

25 Increasing evidence suggests cortical involvement in the control of human gait.
26 However, the nature of corticospinal interactions remains poorly understood. We
27 performed time-frequency analysis of electrophysiological activity acquired during
28 treadmill and overground walking in 22 healthy, young adults. Participants walked at
29 their preferred speed (4.2, SD 0.4 km h⁻¹), which was matched across both gait
30 conditions. Event-related power, corticomuscular coherence (CMC) and inter-trial
31 coherence (ITC) were assessed for EEG from bilateral sensorimotor cortices and EMG
32 from the bilateral tibialis anterior (TA) muscles. Cortical power, CMC and ITC at theta,
33 alpha, beta and gamma frequencies (4-45 Hz) increased during the double support phase
34 of the gait cycle for both overground and treadmill walking. High beta (21-30 Hz) CMC
35 and ITC of EMG was significantly increased during overground compared to treadmill
36 walking, as well as EEG power in theta band (4-7 Hz). The phase spectra revealed
37 positive time lags at alpha, beta and gamma frequencies, indicating that the EEG
38 response preceded the EMG response. The parallel increases in power, CMC and ITC
39 during double support suggest evoked responses at spinal and cortical populations rather
40 than a modulation of ongoing corticospinal oscillatory interactions. The evoked
41 responses are not consistent with the idea of synchronization of ongoing corticospinal
42 oscillations, but instead suggest coordinated cortical and spinal inputs during the double
43 support phase. Frequency-band dependent differences in power, CMC and ITC between
44 overground and treadmill walking suggest differing neural control for the two gait

45 modalities, emphasizing the task-dependent nature of neural processes during human
46 walking.

47 **New & Noteworthy**

48 We investigated cortical and spinal activity during overground and treadmill walking in
49 healthy adults. Parallel increases in power, CMC and ITC during double support
50 suggest evoked responses at spinal and cortical populations rather than a modulation of
51 ongoing corticospinal oscillatory interactions. These findings identify
52 neurophysiological mechanisms that are important for understanding cortical control of
53 human gait in health and disease.

54

55 **Keywords:** human gait, corticomuscular coherence, ambulatory EEG, neural
56 oscillations, time-frequency analysis

57

58 **Introduction**

59 The control of human locomotion has commonly been thought to be driven by
60 spinal and subcortical neural circuits. This assumption has been primarily based on
61 animal studies, which show that cortical networks are only involved in generating
62 locomotor activity in animals during more demanding walking tasks, such as precision
63 stepping or obstacle avoidance (Armstrong 1988; Drew et al. 2008; Grillner 1985).
64 Increasing evidence from human neuroimaging studies suggests that cortical structures
65 contribute to the control of simple, steady-state human gait (Fukuyama et al. 1997;
66 Gwin et al. 2011; la Fougère et al. 2010; Miyai et al. 2001; Petersen et al. 2012; Seeber
67 et al. 2014). However, the nature of corticospinal interactions that underlie this control
68 remains poorly understood.

69 In recent years ambulatory electroencephalography (EEG) has been increasingly
70 used to investigate cortical and corticospinal sensorimotor processes during walking in
71 humans (Artoni et al. 2017; Bradford et al. 2016; Bruijn et al. 2015; Bulea et al. 2015;
72 Gwin et al. 2011; Knaepen et al. 2015; Luu et al. 2017; Oliveira et al. 2017b; Petersen et
73 al. 2012; Seeber et al. 2014; Seeber et al. 2015; Severens et al. 2012; Sipp et al. 2013;
74 Storzer et al. 2016; Wagner et al. 2016; Wagner et al. 2012; Wagner et al. 2014;
75 Winslow et al. 2016). Time-frequency analysis revealed that cortical oscillations and
76 corticospinal interactions are modulated relative to the gait cycle at theta (4-7 Hz), alpha
77 (8-12 Hz), beta (13-30 Hz) and gamma (>30 Hz) frequencies. However, there are
78 considerable discrepancies in the precise temporal and spectral patterns of cortical
79 dynamics, probably due to the wide variety of walking tasks used (e.g. treadmill
80 walking at different speeds, on gradients, with additional gait-stability-challenging

81 tasks, with robotic assistance). For instance, beta oscillations were found to be enhanced
82 during the double support phases of the gait cycle (event-related synchronization, ERS)
83 and to be suppressed during the swing and single support phases (event-related
84 desynchronization, ERD) (Artoni et al. 2017; Bradford et al. 2016; Bruijn et al. 2015;
85 Bulea et al. 2015; Cheron et al. 2012; Gwin et al. 2011; Knaepen et al. 2015; Severens
86 et al. 2012). In contrast, other groups observed ERS at 24-40 Hz (low gamma) during
87 early and mid-swing, and ERD towards the end of the swing phase and during double
88 support (Seeber et al. 2014; Seeber et al. 2015; Storzer et al. 2016; Wagner et al. 2012;
89 Wagner et al. 2014).

90 There are also some initial reports which suggest that these cortical oscillations
91 are transmitted to spinal motoneurons during walking in humans (Artoni et al. 2017;
92 Brantley et al. 2016; Petersen et al. 2012; Winslow et al. 2016). In nine participants,
93 Petersen *et al.* (2012) showed corticomuscular coherence (CMC) between
94 electroencephalographic (EEG) and electromyographic (EMG) signals from the tibialis
95 anterior muscle (TA) at 8–12 Hz and 24–40 Hz during walking. CMC was observed
96 approximately 400 ms prior to heel strike at two different walking speeds (1 km h⁻¹ and
97 3.5–4 km h⁻¹). It is uncertain which exact phase of the gait cycle this would correspond
98 to, as 400 ms before heel strike would coincide with different phases of the gait cycle at
99 these two walking speeds (Castermans and Duvinage 2013). The authors suggested that
100 CMC at 24-40 Hz during walking represents an efferent drive from cortex to spinal
101 motoneurons, as they observed a negative imaginary part of coherency indicating a
102 positive time lag from EEG to EMG (Petersen et al. 2012); however, the absolute time
103 lag was not investigated. Recently, Artoni and colleagues (2017) reported a descending
104 connectivity from motor cortex to leg muscles during undemanding, steady-state

105 treadmill walking, which was strongest for muscles of the swing leg but also present for
106 muscles of the stance leg.

107 The vast majority of previous studies investigating gait-related cortical
108 oscillations have been conducted on standard, motorized treadmills. Overground
109 walking, however, has been shown to differ from treadmill walking dynamically and
110 mechanically (Alton et al. 1998; Arsenault et al. 1986; Carpinella et al. 2010; Chiu et al.
111 2015; Dingwell et al. 2001; Lee and Hidler 2008; Ochoa et al. 2017; Riley et al. 2007;
112 White et al. 1998). For example, treadmill walking has been found to reduce kinematic
113 variability (Chiu et al. 2015; Dingwell et al. 2001), increase local dynamic stability
114 (Dingwell et al. 2001), affect inter-limb coordination (Carpinella et al. 2010), modify
115 lower limb muscle activation patterns, and joint moments and powers (Lee and Hidler
116 2008). These observations suggest that sensorimotor control of locomotion may vary
117 between these two gait modalities, potentially affecting processes at the level of the
118 cortex.

119 In the present study, we investigate cortical sensorimotor oscillations and
120 corticospinal interactions during treadmill and overground walking in a large sample of
121 healthy, young adults. By examining changes in cortical power and CMC during the
122 gait cycle, we investigate the temporal and spectral profile of corticospinal interactions
123 during human walking. In addition, we investigate inter-trial coherence (ITC; Delorme
124 and Makeig 2004) to assess the phase dynamics associated with the changes in spectral
125 power. By comparing power and phase changes we can distinguish whether event-
126 related components result from an evoked activation that is superimposed on the
127 ongoing background activity (hence, an additive response independent from ongoing
128 activity; evoked response), or whether ongoing activity is altered by means of changes

129 in amplitude and/or phase (i.e. corticospinal interactions modulate the phase of ongoing
130 activity; induced response) (Boonstra et al. 2006; Makeig et al. 2004). Finally, the
131 ‘constant phase shift plus constant time lag model’ (Mima and Hallett 1999) was used
132 to estimate the time lag from the CMC phase spectra and investigate the time lag of
133 corticospinal interactions. Together, these spectral analyses will elucidate the nature of
134 corticospinal dynamics involved in human gait.

135 **Materials and Methods**

136 Twenty-four healthy young adults (mean (SD), age 25.9 (3.2) years, height 170.4
137 (9.5) cm, weight 68.8 (12.1) kg; 12 men and 12 women) participated in the study. All
138 experimental protocols were approved by the Human Research Ethics Committee of
139 Queensland University of Technology (#1300000579) in accordance with the
140 Declaration of Helsinki, and all participants gave written informed consent prior to
141 participation.

142 **Experimental protocol**

143 Participants performed 12-14 minutes of overground walking and approximately
144 seven minutes of treadmill walking at their preferred walking speed (3.3 – 4.8 km h⁻¹).
145 The order of treadmill and overground walking was randomised across participants. The
146 first two minutes of each trial served as familiarisation period and was not included in
147 the analysis. In the overground condition, participants walked back and forth along a
148 straight path (approximately 14 m) on a firm surface in the gait laboratory and turned at
149 each end of the room. The turning sections, including acceleration at the beginning of

150 the straight-line path and deceleration at the end (approximately 2.4 m), were labelled
151 by the examiner and not included in further analyses, leaving 8.9 m of straight-line
152 walking for further analysis. In order to obtain a similar amount of straight-line walking
153 data in the overground condition, participants were required to walk for a longer
154 duration (12-14 min) than in the treadmill condition (7 min). Treadmill walking was
155 performed on a conventional treadmill (Nautilus, Pro Series). Both walking conditions
156 were completed barefoot. Participants were instructed not to blink excessively, to
157 reduce swallowing and to relax their face, jaw, and shoulder muscles during the data
158 acquisition periods in order to minimise EEG artefacts. Participants rested for five
159 minutes between overground and treadmill walking in order for residual walking-
160 specific after-motion-effects to dissipate and to prevent fatigue.

161 Gait velocity was individually matched for treadmill and overground walking. To
162 this end, participants completed a 'pre-trial' (overground) of approximately three
163 minutes before the actual experiment commenced in order to determine their preferred
164 walking speed. Their mean walking velocity during the pre-trial was used to set the
165 treadmill belt speed and to monitor and maintain the participants' walking speed
166 consistent during the overground walking condition. If the participant did not comply
167 with the pre-determined mean walking speed during the overground condition, they
168 were instructed to walk faster/slower.

169 **Data acquisition**

170 Paired bipolar surface EMG (Ag-AgCl electrodes, 1 cm² recording area, 2 cm
171 between poles) was recorded from the belly of the left and right TA. The TA was
172 chosen as recording site based on previous reports of CMC and intra-muscular

173 coherence during walking (Halliday et al. 2003; Petersen et al. 2012). EMG signals
174 were filtered at 1-1000 Hz. Simultaneous EEG recordings were made using water-based
175 AgCl electrodes placed on the scalp at 10 cortical sites according to the international 10-
176 20 standard (P3, P4, C3, Cz, C4, F7, F3, Fz, F4, F8) using a 24-electrode cap (Headcap
177 for water-based electrodes, TMSi, The Netherlands). Combined mastoids (A1, A2) were
178 used as reference. The ground electrode was situated on the wrist using a wristband
179 (TMSi, The Netherlands). EEG signals were filtered at 1-500 Hz. Footswitches were
180 attached onto the participants' sole at the heel and the big toe of both feet. Synchronized
181 EEG, EMG, and footswitch signals were recorded with a wireless 32-channel amplifier
182 system (TMSi Mobita, The Netherlands) and sampled at 2 kHz. The recording system
183 and wireless transmitter were placed in a belt bag and tied around the participants'
184 waist.

185 **Data analysis**

186 All processing of data and spectral analyses were performed in MATLAB (2017a)
187 using custom written routines.

188 **Temporal gait parameters**

189 Temporal gait parameters were extracted from the footswitch recordings. Time
190 points of heel strike and toe-off for both feet were extracted and several gait parameters
191 were calculated including stride time, step time, stride- and step time variability,
192 cadence, swing phase, stance phase, single- and double-support time. Time points of
193 heel strike and toe-off were extracted from the digital output signal of the TMSi Mobita
194 system. The channels of the amplifier system used for the footswitches have a default
195 value of approximately -2.04V when 'off' and -1.14V when 'on'; the threshold for a

196 gait cycle event (heel strike or toe-off) was set to -1.64V. Walking velocity was
197 calculated based on the time it took participants to complete the 8.9 m of straight-line
198 walking during overground walking.

199 **Data pre-processing and artefact removal**

200 Prior to spectral analysis, electrophysiological data were pre-processed and
201 artefacts were removed according to the following steps/processes. EEG channels were
202 visually inspected and segments with excessive noise (large-amplitude movement
203 artefacts, EMG activity) were rejected. Next, EEG signals were band-pass filtered (2nd
204 order Butterworth, 0.5-70 Hz) and re-referenced to a common average reference (re-
205 referencing was performed in EEGLAB version 13.6.5, Delorme and Makeig 2004). A
206 common average reference in the post-processing steps has been shown to minimize
207 motion artefacts in EEG signals (Snyder et al. 2015). EEG recordings during
208 overground walking were truncated to the straight-line walking segments (turning
209 segments were removed). Subsequently, independent component analysis (ICA) was
210 performed on the concatenated segments using the infomax ICA algorithm implemented
211 in EEGLAB. Independent components containing eye blink, muscle, or movement
212 artefacts were removed from the data (on average 3.7 components were removed per
213 participant); the remaining components were retained and projected back onto the
214 channels. Components were assessed based on their topographical projections, power
215 spectra and time series. For instance, independent components were classified as ocular
216 artefacts when the topographical map showed a far-frontal projection, the median
217 frequency was below 3 Hz and the time course showed positive peaks lasting a few
218 tenths of a second at ≤ 3 Hz intervals (Delorme and Makeig 2011).

219 A bipolar EEG montage was used to assess cortical activity from bilateral
220 sensorimotor cortices: C3-F3 for the left sensorimotor cortex, and C4-F4 for the right
221 sensorimotor cortex (cf. Long et al. 2015). A differential recording between the
222 electrode pairs is most sensitive to activity locally generated between the electrode pairs
223 and suppresses more distant activity. Hence, it can be used to minimize artefacts similar
224 to a common reference approach (e.g. Petersen et al. 2012; Snyder et al. 2015).

225 EMG data were high-pass filtered (4th order Butterworth, 10 Hz cut-off) and full-
226 wave rectified using the Hilbert transform. There is some discussion on the use of EMG
227 rectification for the estimation of CMC (Halliday and Farmer 2010; McClelland et al.
228 2012; Neto and Christou 2010). For assessing CMC at low force levels, it has been
229 shown that rectification is appropriate (Boonstra and Breakspear 2012; Farina et al.
230 2013; Ward et al. 2013). We therefore rectified the EMG signals, as walking qualifies as
231 low force movement. Moreover, rectification of EMG signals in the process of
232 calculating CMC has been applied in previous ambulatory CMC studies (Petersen et al.
233 2012).

234 After rectification, EMG signals were demodulated to avoid spurious coherence
235 estimates resulting from periodic changes in EMG amplitude (Boonstra et al. 2009).
236 Walking periodically activates the muscles and results in a rapid increase in EMG
237 amplitude during each gait cycle. These fluctuations in EMG amplitude were removed
238 by demodulating the EMG signal using the Hilbert transform to obtain the instantaneous
239 phase θ of the rectified EMG signal. The demodulated EMG signal y can be defined as
240 the cosine of the instantaneous frequency or phase $y = \cos\{\theta\}$, where y has amplitude 1
241 and the same instantaneous phase as the original rectified EMG signal (Boonstra et al.
242 2009).

243 Spectral analysis

244 Time-frequency analysis was used to assess changes in corticospinal interactions
245 during walking for two bipolar EEG signals (C4-F4, C3-F3) and rectified and
246 demodulated EMG signals of bilateral TA muscles (TA_l, TA_r) with respect to heel
247 strike of the left and right foot. To this end, EEG and EMG signals were segmented into
248 $L = 220$ segments of length $T = 1000$ ms (-800 to +200 ms with respect to heel strike of
249 the right or left foot) for each participant and condition. Heel strike served as reference
250 point ($t = 0$) in the gait cycle to which all segments were aligned. Event-related power
251 spectra and coherence were computed across the 220 segments using a 375-ms Hanning
252 window and a sliding window method with increments of 25 ms. The window length
253 was determined after visual inspection of different window settings with simulated data
254 and experimental data of a representative participant, showing that a window of 375 ms
255 optimised the trade-off between spectral and temporal resolution.

256 Time-frequency power is hence defined as:

$$p_{xx}(t, f) = \frac{1}{L} \sum_1^L |X_s(t, f)|^2,$$

257 where $X_s(t, f)$ is the Fourier transform of the s^{th} segment of signal x , t denotes the time
258 relative to the heel strike, f the discrete frequency and L the number of segments.
259 Likewise, the cross-spectrum is defined as

$$p_{xy}(t, f) = \frac{1}{L} \sum_1^L X_s(t, f) Y_s(t, f)^*,$$

260 where ‘*’ indicates the complex conjugate. Event-related power was expressed as
261 percentage change from the average by subtracting and dividing by the mean power
262 across the time interval separately for each frequency (Boonstra et al. 2007).

263 Complex-valued time-frequency coherency is then defined as:

$$C_{xy}(t, f) = \frac{p_{xy}(t, f)}{\sqrt{(p_{xx}(t, f) p_{yy}(t, f))}},$$

264 and event-related coherence (Boonstra et al. 2009; Delorme and Makeig 2004) as:

$$coh_{xy}(t, f) = |C_{xy}(t, f)|^2 = \frac{|p_{xy}(t, f)|^2}{p_{xx}(t, f) p_{yy}(t, f)}.$$

265 Inter-trial coherence (ITC) can be quantified by averaging the complex-valued Fourier
266 decomposition of x over the L segments and normalising it by the auto-spectrum:

$$ITC_x(t, f) = \frac{\left| \frac{1}{L} \sum_1^L X_s(t, f) \right|^2}{p_{xx}(t, f)}.$$

267 Similar to coherence, ITC is bound between 0 and 1, where 0 indicates the absence of
268 synchronization between the data and the time-locking events and 1 perfect
269 synchronization, i.e., perfect phase reproducibility across trials at a given latency
270 (Delorme and Makeig 2004).

271 Power and coherence spectra were computed for each participant during
272 overground and treadmill walking, and subsequently averaged across participants to
273 render the grand-average for each estimate and condition. Additionally, event-related
274 EMG envelopes were computed using filtered and rectified EMG data.

275 To investigate the timing relationship between EEG and EMG activity, we
276 assessed the phase difference between both signals (Halliday et al. 1995). The time lag
277 and phase offset between two signals can be determined from the phase spectra. That is,
278 a constant time lag between two signals results in a linear trend in the phase difference
279 across frequencies (Mima and Hallett 1999). To estimate the time lag from the phase

280 spectra, we fitted a line to the phase spectrum across the frequency range at which
281 significant coherence was observed, and the time lag can be directly calculated from the
282 slope of the regression line (Mehrkanoon et al. 2014; Raethjen et al. 2002). Time lags
283 were separately calculated for different frequency bands and conditions. To this end,
284 complex-valued coherency was averaged across C3F3-TAr and C4F4-TAl to improve
285 the signal-to-noise ratio. Subsequently, the phase spectra were extracted from the
286 averaged coherency estimates, and time lags were calculated for theta, alpha, low beta,
287 high beta and gamma frequency ranges.

288 **Statistical analysis**

289 Significance level (α) was set at 0.05 for all statistical analyses.

290 Paired sample t-tests (SPSS, version 23) were used to compare gait parameters
291 across conditions (overground, treadmill).

292 To assess whether the coherence estimates were statistically significant in
293 individual participants, confidence intervals (CI) were constructed based on the number
294 of segments included in the analysis. The 95% confidence interval CI was estimated as
295 (Amjad et al. 1997)

$$296 \quad CI = 1 - (\alpha)^{1/(L-1)},$$

297 where α defines the significance threshold and L the number of segments. Here
298 α is set to 0.05 and the resulting CI is hence $1 - (0.05)^{1/(220-1)} = 0.0136$. The
299 same CI was also used for ITC.

300 A two-stage summary statistics approach was used to assess statistical
301 significance of time–frequency coherence at group level. First, magnitude-squared
302 coherence of individual participants was transformed to z-scores using a parametric

303 approach (Halliday et al. 1995). To this end, we first computed the p-values of the
304 coherence values. The p-value of coherence can be estimated as

$$305 \quad p = 1 - (1 - \text{coh})^{(L-1)},$$

306 where *coh* is magnitude-squared coherence (Halliday et al. 1995). Then we used the
307 standard normal distribution to convert p-values into z-scores, which have an expected
308 value of 0 and a standard deviation of 1 under the null hypothesis (EEG and EMG
309 signals are independent). Second, a one-sample t-test was used to test whether the
310 individual z-scores were significantly different from zero (Mehrkanoon et al. 2014).
311 This approach was used to test statistical significance of CMC and ITC.

312 Linear mixed models (LMM) were used to compare the repeated measures of z-
313 transformed coherence across conditions (overground, treadmill). Mean z-transformed
314 coherence over salient time-frequency windows was used for the analysis. Five time-
315 frequency windows were identified: Double support (0 to 125 ms at/after heel strike) at
316 (i) theta (4-7 Hz), (ii) alpha (8-12 Hz), (iii) lower beta (13-20 Hz), (iv) higher beta (21-
317 30 Hz), and (v) gamma frequencies (31-45 Hz). Hence, five separate LMMs were
318 completed (one for each frequency band). Statistically significant main effects were
319 followed up with post-hoc comparisons (t-tests) and family-wise error rate was
320 controlled by using a Bonferroni adjustment for multiple comparisons. The fixed effect
321 factor included in the model was condition; data of both left and right EEG-EMG pairs
322 (C3F3-TAr, C4F4-TAl) were included to compare overground versus treadmill gait. A
323 random effect for participant (i.e. using the participant identification number) was
324 included in the model, which takes into account the repeated coherence measures
325 among participants. The LMM analysis was performed in SPSS (version 23). The same
326 model was used to compare EEG power and ITC across conditions (overground,

327 treadmill). Mean normalized PSD over the salient time-frequency windows per
328 participant was used for the analysis.

329 An intercept-LMM with a fixed effect factor for condition was used to compare
330 the time lags of the different frequency bands against zero, and across overground and
331 treadmill walking. A significant intercept represents a rejection of the null hypothesis
332 and indicates a non-zero time lag between EEG and EMG signals at group level. A
333 significant effect for condition indicates a difference in time lag between overground
334 and treadmill walking.

335 **Results**

336 Data from two participants were excluded from the spectral analysis (i.e. for all
337 spectral outcome measures: power, coherence and phase) due to excessive EEG
338 artefacts across all channels and conditions (large-amplitude movement artefacts
339 ($>300\mu\text{V}$) occurring with regular rhythmicity in each gait cycle throughout the entire
340 record). Another two datasets were excluded during treadmill walking, because fewer
341 than 100 left heel strike triggers were extracted. Thus, group mean estimates for spectral
342 analyses relative to heel strike of the left foot during treadmill walking (i.e. C4F4 for
343 power, and C4F4-TA1 for coherence and phase) were based on $n = 20$ participants. All
344 other spectral estimates (C3F3-TAr coherence/phase and C3F3 power overground and
345 treadmill, C4F4-TA1 coherence/phase and C4F4 overground) were based on $n = 22$
346 participants.

347 **Temporal gait parameters**

348 Participants were instructed to walk at their preferred speed, which was matched
349 across both gait conditions. Mean walking speed was not significantly different between
350 overground and treadmill walking ($p = 0.36$). However, walking speed values were
351 missing for three participants; hence, the group mean estimate was based on $n = 19$
352 participants. Table 1 presents all temporal gait parameters during overground and
353 treadmill walking extracted from the footswitch recordings.

354 Most temporal gait parameters were not significantly different between
355 overground and treadmill walking: including duration of step time, step and stride time
356 variability, swing, single and double support phases. However, stride time was
357 significantly longer during overground than during treadmill walking ($p = 0.007$), and
358 there was a trend towards an extended stance phase during overground walking ($p =$
359 0.054). Moreover, participants walked at a higher cadence on the treadmill than they did
360 overground ($p = 0.012$).

361 **EMG envelope**

362 Figure 1A and B shows the event-related EMG envelopes for the right and left TA
363 during overground and treadmill walking. The pattern shows increased amplitude
364 during early swing (around -300 ms prior to heel strike), as well as during late swing
365 and early stance (-100 ms prior to $+100$ ms after heel strike). During mid swing (around
366 -200 ms prior to heel strike) the amplitude decreased. The envelope is marked by a
367 double peak at the time point of heel strike ($t = 0$) when the foot is fully dorsiflexed and
368 at 60 ms after heel strike (early double support). The amplitude increased during early

369 swing already commenced before toe-off of the swing leg. We present single participant
370 data in the appendix.

371 **Event-related power**

372 The amplitude modulations of cortical activity revealed a different pattern.
373 Increased EEG power was observed across a range of frequencies during double
374 support, while power reduced during the swing and single support phases (Figure 1C to
375 F). The greatest power increase was observed during double support between
376 approximately 15 to 25 Hz, with an increase of up to 55% relative to the average across
377 the whole gait cycle.

378 The statistical comparison using LMM revealed that EEG power during double
379 support in the theta band was significantly greater during overground compared to
380 treadmill walking ($F(1, 63.9) = 5.04, p = 0.03$; Figure 2A). The increase in theta power
381 was 29.7% during double support for overground and 15.2% for treadmill walking; the
382 estimated mean difference was 14.5% [95% CI: 1.6-27.4]. No significant differences (p
383 ≥ 0.14) between overground and treadmill walking were observed for the other
384 frequency bands (Figure 2A).

385 **Corticomuscular coherence**

386 During both gait conditions CMC increased during the double support phase of
387 the gait cycle at frequencies between 0 to approximately 45 Hz and little or no CMC
388 was observed during the swing and single support phase (Figure 3). During the double
389 support phase, CMC decreased at higher frequencies showing the highest CMC for
390 frequencies <10 Hz, medium CMC for frequencies 11-20 Hz, lowest CMC for

391 frequencies >25 Hz. CMC was statistically significant during double support in all
392 frequency bands for both sides/channels and gait conditions ($p < 0.02$).

393 The statistical comparison of the gait conditions using LMMs revealed that CMC
394 in the high beta band was significantly greater during overground compared to treadmill
395 walking ($F(1, 63.7) = 4.44$, $p = 0.04$; Figure 2B). Grand-average z-transformed high
396 beta coherence was 1.90 during overground and 1.31 during treadmill walking; the
397 estimated mean difference was 0.59 [95% CI: 0.03-1.14]. No significant differences
398 between overground and treadmill walking were observed in the other frequency bands
399 ($p \geq 0.06$).

400 **Inter-trial coherence**

401 EEG revealed a significant ITC increase during the double support phases of the
402 gait cycle at frequencies between 4 to 50 Hz, and little or no ITC during the swing and
403 single support phases (Figure 4). During the double support phase, ITC decreased at
404 higher frequencies showing the highest ITC for frequencies <10 Hz, medium ITC for
405 frequencies 11-30 Hz, lowest ITC for frequencies >30 Hz. This pattern was similar for
406 overground and treadmill gait, and for left and right sensorimotor cortices. ITC of
407 bilateral EMG revealed a similar pattern (Figure 5): ITC was largest during the double
408 support phases.

409 EEG and EMG ITC was statistically significant during double support in all
410 frequency bands for both sides/channels and gait conditions ($p < 0.0001$).

411 The statistical comparison of the gait conditions using LMMs revealed that ITC of
412 the left and right SMC during double support was not significantly different between
413 overground and treadmill walking for any of the frequency bands ($p \geq 0.25$; Figure 2C).

414 ITC of the left and right TA was significantly greater during overground compared to
415 treadmill walking in the high beta band ($F(1, 63.14) = 7.79, p = 0.007$; Figure 2D).
416 Grand-average high-beta ITC was 0.15 during overground and 0.11 during treadmill
417 walking; the estimated mean difference was 0.03 [95% CI: 0.009-0.056]. No significant
418 differences between overground and treadmill walking were observed in the other
419 frequency bands ($p \geq 0.06$).

420 **Phase spectra**

421 The time delay between EEG and EMG was estimated during overground and
422 treadmill walking separately in each frequency band (theta, alpha, lower beta, higher
423 beta, gamma; Figure 6). We extracted the coherence spectrum in the middle of the
424 double support phase ($t = 50$ ms) and determined for each participant the frequency bins
425 at which CMC was significant. A linear line was fitted to these frequency bins of the
426 corresponding phase spectra and the time lag was estimated from the slope of the fitted
427 line (see Figure 6A and B for an example in the lower beta band).

428 Statistical analyses of time lag revealed that time lag during double support was
429 greater than zero in the alpha ($F(1, 33) = 13.3, p = 0.0009$), low beta ($F(1, 39) = 6.88, p$
430 $= 0.012$), high beta ($F(1, 25) = 19.4, p = 0.0002$), and gamma bands ($F(1, 17) = 7.84, p$
431 $= 0.012$), but not in the theta band ($p = 0.84$). This indicates that EEG signals were
432 leading EMG signals in alpha, beta and gamma frequency bands. The grand-average
433 time lag was 30.0 ms [95% CI: 13.3-46.8] in the alpha band, 11.4 ms [95% CI: 2.6-
434 20.8] in low beta, 26.5 ms [95% CI: 14.1-38.9] in high beta, 18.3 ms [95% CI: 4.5-32.0]
435 in the gamma band (Figure 6C). No significant differences in time lag were observed
436 between overground and treadmill walking ($p \geq 0.15$).

437 **Discussion**

438 Spectral measures (power, CMC and ITC) were examined during overground and
439 treadmill walking to investigate corticospinal dynamics during both gait conditions.
440 Significant CMC at theta, alpha, beta and gamma frequencies (4-45 Hz) was found
441 between the sensorimotor cortex and the contralateral TA muscle during the double
442 support phase. CMC was largely absent during the swing phase. Similarly, EEG power
443 and ITC increased in these frequency bands during double support and decreased during
444 swing for both gait conditions. CMC and ITC of EMG was significantly enhanced in the
445 high beta band during overground compared to treadmill walking, as well as EEG
446 power in the theta band. Alpha, beta and gamma CMC during double support showed a
447 time lag from EEG to EMG, suggesting that cortical activity was leading muscle
448 activity. Most temporal gait parameters were not significantly different between
449 overground and treadmill walking, except stride time (longer overground) and cadence
450 (lower overground).

451 **Phasic activity during double support**

452 For both overground and treadmill walking, we found that EEG power, CMC and
453 ITC increased during the double support phase of the gait cycle and decreased during
454 swing/single support. Cortical and corticospinal synchronization increased at a broad
455 frequency range, including theta, alpha, beta and gamma frequencies. These results
456 highlight that cortical and corticospinal activity is modulated dependent on the phase of
457 the gait cycle and suggest that the cortex is intermittently involved in controlling human
458 gait.

459 The cortical power fluctuations during overground and treadmill walking
460 observed in this study closely resemble those previously reported in ambulatory EEG
461 studies conducted on a treadmill. A number of studies found increased power over
462 sensorimotor cortical areas at the end of stance and during double support, and
463 decreased power during the swing/single support phase (Artoni et al. 2017; Bradford et
464 al. 2016; Bruijn et al. 2015; Bulea et al. 2015; Cheron et al. 2012; Gwin et al. 2011;
465 Knaepen et al. 2015; Luu et al. 2017; Oliveira et al. 2017b; Severens et al. 2012).
466 Notably, one previous study (Bulea et al. 2015) reported similar changes in cortical
467 power to those in the current study during walking on a user-driven treadmill, a
468 condition which simulates overground walking more closely than walking on a
469 standard, motorized treadmill. However, other studies reported increased power during
470 the swing phase and reduced power during double support (Seeber et al. 2014; Seeber et
471 al. 2015; Storzer et al. 2016; Wagner et al. 2012; Wagner et al. 2014). Walking tasks in
472 these studies included treadmill walking in a robotic driven gait orthosis (Seeber et al.
473 2014; Seeber et al. 2015; Wagner et al. 2012; Wagner et al. 2014) and overground
474 walking (Storzer et al. 2016). While robot assisted walking is quite different from
475 steady-state treadmill walking, which may help to explain discrepant findings, the
476 changes in cortical power found during overground walking by Storzer *et al.* (2016)
477 differ substantially from our results. In their study, participants were required to walk at
478 a cadence of 40 strides per minute (although no audio-visual cues were provided to
479 ensure compliance) and walking speed was not kept constant throughout the trial,
480 whereas our participants chose their own cadence for each gait condition
481 (approximately 55 strides per minute) and walking speed was kept constant ($\sim 4 \text{ km h}^{-1}$).

482 The time-frequency profiles of CMC largely match the profiles of cortical
483 oscillations. To our knowledge, only one study (Petersen et al. 2012) and two case-
484 reports (Brantley et al. 2016; Winslow et al. 2016) have previously investigated CMC
485 during walking. Petersen et al. (2012) found significant CMC between motor cortex and
486 TA at 8-12 and 24-40 Hz during treadmill walking, which partly overlap with the
487 frequency ranges in the current study. While all studies show corticospinal interactions
488 during steady-state walking in humans, the temporal profiles of CMC may differ: We
489 found CMC mainly during double support, whereas Petersen et al. (2012) observed
490 CMC ~400 ms prior to heel strike at two different walking speeds (1 km h⁻¹ and 3.5–4
491 km h⁻¹). It is uncertain which phase of the gait cycle this exactly corresponds to, as 400
492 ms before heel strike would coincide with different phases of the gait cycle at these two
493 walking speeds (Castermans and Duvinage 2013). A systematic investigation of CMC
494 at different walking speeds may help to resolve the timing of intra-stride modulations of
495 CMC, as the activations patterns of the TA muscle are strongly modulated by walking
496 speed (den Otter et al. 2004). The case-reports by Winslow et al. (2016) and Brantley et
497 al. (2016) investigated CMC during overground walking in a single subject over a
498 single gait cycle: Winslow et al. (2016) observed CMC between motor cortex and TA at
499 approximately 18-23 Hz just after heel strike and just after toe-off, whereas Brantley et
500 al. (2016) reported CMC between motor cortex and TA at frequencies below 5 Hz
501 throughout the gait cycle. Artoni and colleagues (2017) recently showed a descending
502 connectivity from motor cortical regions to different leg muscles during the swing phase
503 of steady-state treadmill walking. This unidirectional, top-down connectivity was
504 strongest for muscles of the swing leg but also present for muscles of the stance leg
505 during the swing phase. Corticomuscular connectivity was stronger for the TA muscles

506 (of both swing and stance leg) than for other more proximal muscles. However,
507 corticomuscular connectivity was only assessed during the swing phase but not during
508 other phases of the gait cycle (e.g. stance or double support).

509 The TA EMG envelopes we present in Figure 1A and B (and in Figure 7 in the
510 Appendix) are consistent with previous reports in the literature (Campanini et al. 2007;
511 Courtine and Schieppati 2003; Halliday et al. 2003; Perry 1992; Sutherland 2001; Yang
512 and Winter 1984). Overall, the temporal profiles of our EMG envelopes reveal a well-
513 identified double burst in which the TA is first activated during the onset of swing and
514 then again at the end of swing around heel strike. At the time of heel strike the TA is
515 maximally dorsiflexed within the gait cycle, and after heel strike the TA is performing
516 an eccentric contraction (plantarflexion) which controls foot drop. As the increase of
517 CMC during double support overlaps with the second burst of TA activity, CMC may
518 potentially be involved in maintaining balance during gait by controlling plantarflexion
519 after heel strike. It is interesting that in hemiplegic subjects tibialis anterior activity
520 during swing phase was not affected while they tended to lack the normal second peak
521 of activity at initial foot contact (Burridge et al. 2001). Further experimental
522 investigation of CMC between cortex and leg muscles other than the TA during walking
523 may help to resolve the functional role of CMC during gait. If CMC reflects the
524 descending drive to the muscle, one would expect to find CMC at different phases of
525 the gait cycle for different leg muscles. However, it is worthwhile noting that during
526 dynamic ankle movements beta CMC has been observed during dorsiflexion for two
527 antagonistic muscles (Yoshida et al. 2017).

528 **Evoked versus induced activity**

529 In addition to the increase in power and CMC, we also observed increased ITC
530 during the double support phases at a broad range of frequencies (theta, alpha, beta and
531 gamma frequencies). ITC quantifies phase locking of the EEG and EMG signals to the
532 time-locking events (Makeig et al. 2004), in this case the heel strike. Phase locking has
533 been widely used to investigate the neural mechanisms that generate event-related brain
534 responses (Fell et al. 2004; Makeig et al. 2004; Shah et al. 2004). Two opposing
535 theories have been discussed that may generate time-locked components: ‘phase
536 resetting’ in which a cortical input resets the phase of ongoing EEG rhythms (induced
537 activity) and ‘evoked responses’ in which input evokes an additive, neural-population
538 response that is independent from ongoing activity. Importantly, induced and evoked
539 activity are not distinguished based on whether the input is generated by a stimulus, but
540 whether it reflects a change in ongoing activity or a response that is linearly added to
541 ongoing activity. A key difference between the phase resetting and evoked models is
542 that an evoked response will be accompanied by an induced increase in power, whereas
543 such an increase is absent in phase resetting (Fell et al. 2004). Although the distinction
544 between evoked and induced activity is not trivial (Mazaheri and Jensen 2010; Ritter
545 and Becker 2009), the parallel increase in power and ITC observed in the current study
546 is most compatible with an evoked response (cf. Tallon-Baudry et al. 1996). Following
547 this interpretation, the time-frequency profile of power and ITC changes would reflect
548 the waveform of the additive response evoked during the double support phase. The
549 waveform of the evoked EMG response can be observed in the EMG envelopes
550 showing a double peak at the time point of heel strike ($t = 0$) and at 60 ms after heel

551 strike. This corresponds to a $1000/60 = 16.7$ Hz oscillation, which is also the frequency
552 at which a peak in ITC is observed (Figure 4).

553 If the event-related changes indeed reflect an evoked response, this would require
554 a reinterpretation of the observed increase in EEG power during the double support
555 phases. Changes in cortical power are often interpreted as event-related synchronization
556 and desynchronization (ERS/ERD), which is thought to reflect a change in the local
557 synchronization of a neuronal ensemble (Pfurtscheller and Lopes da Silva 1999). As
558 such, ERS and ERD reflect an induced response of ongoing activity rather than an
559 additive response and would hence not be accompanied by phase locked activity
560 (Tallon-Baudry et al. 1996). As the changes in spectral power observed here closely
561 resemble those previously reported in ambulatory EEG studies (Artoni et al. 2017;
562 Bradford et al. 2016; Bruijn et al. 2015; Bulea et al. 2015; Cheron et al. 2012; Gwin et
563 al. 2011; Knaepen et al. 2015; Luu et al. 2017; Oliveira et al. 2017b; Severens et al.
564 2012), this may require a broader reinterpretation of the cortical dynamics during
565 walking.

566 Likewise, ITC of EMG and EEG suggests an alternative interpretation of the
567 CMC observed during double support. Conventionally, CMC is thought to reflect
568 corticospinal synchronization, where corticospinal interactions synchronizes the activity
569 in the cortex and spine through efferent and afferent pathways (Conway et al. 1995;
570 Petersen et al. 2012). However, the observed ITC shows that cortical and spinal activity
571 is phase locked to an external event, the heel strike, and as such may not reflect true
572 corticospinal synchronization. Synchronization requires two self-sustained oscillators
573 that adjust their rhythms due to weak interactions (Pikovsky et al. 2003). Instead, the
574 current results suggest that comparable responses are evoked at the cortical and spinal

575 level (i.e. represent time-locked responses at cortical and spinal level that are added to
576 ongoing activity). Importantly, these responses did not occur simultaneously. We
577 observed positive time lags between EEG and EMG activity at alpha, beta and gamma
578 frequencies, which indicated that cortical response occurred before the spinal response.

579 **Frequency-specific differences between conditions**

580 We found frequency-specific differences in power, CMC and ITC between
581 overground and treadmill walking. Cortical power during double support was
582 significantly increased at theta frequencies during overground compared to treadmill
583 walking. Similarly, CMC and ITC of EMG at high beta frequencies (21-30 Hz) was
584 significantly enhanced during overground walking. In line with previous research, this
585 highlights that neural activity is affected by the walking task that is performed
586 (Bradford et al. 2016; Bruijn et al. 2015; Bulea et al. 2015; Kline et al. 2016; Knaepen
587 et al. 2015; Lisi and Morimoto 2015; Luu et al. 2017; Oliveira et al. 2017b; Sipp et al.
588 2013; Storzer et al. 2016; Wagner et al. 2016; Wagner et al. 2012; Wagner et al. 2014).
589 For instance, theta ERS in motor cortical regions has been found to be increased during
590 more complex walking tasks, such as walking on a balance beam (Sipp et al. 2013), on a
591 gradient (Bradford et al. 2016), or on an active, user-driven treadmill (Bulea et al.
592 2015). In the context of the present study, this may suggest that overground walking
593 may be more demanding than walking on a motorized, standard treadmill, and hence be
594 accompanied by increased theta ERS. During overground walking participants have to
595 actively track their walking speed and temporospatial gait patterns themselves rather
596 than simply following the treadmill belt speed, which dictates walking speed and
597 influences temporospatial parameters externally. This would indeed be supported by our

598 finding that treadmill walking decreased stride time and increased cadence. Theta ERS
599 has also been linked to critical time points of the gait cycle, such as transitions between
600 stance and swing, as a control strategy of postural stability (Bradford et al. 2016; Sipp et
601 al. 2013). In that sense, the differences in theta ERS we found between overground and
602 treadmill walking may be related to a difference in timing during overground walking.

603 High beta CMC was significantly enhanced during overground walking compared
604 to treadmill walking. To our knowledge, no previous study has compared corticospinal
605 dynamics between locomotor tasks, but only investigated it during treadmill walking
606 (Artoni et al. 2017; Petersen et al. 2012; Winslow et al. 2016). However, a number of
607 studies have assessed cortical oscillations during various gait tasks and have found task-
608 dependent differences in cortical beta power (Bruijn et al. 2015; Bulea et al. 2015;
609 Knaepen et al. 2015; Lisi and Morimoto 2015; Oliveira et al. 2017b; Sipp et al. 2013;
610 Wagner et al. 2016; Wagner et al. 2012; Wagner et al. 2014). These studies have
611 suggested that cortical beta oscillations may be related to controlling gait stability
612 (Bruijn et al. 2015; Sipp et al. 2013), gait adaptations (i.e. step lengthening and
613 shortening, Wagner et al. 2016), sensory processing of the lower limbs (Wagner et al.
614 2012), visuomotor integration (Oliveira et al. 2017b; Wagner et al. 2014), and speed
615 control (Bulea et al. 2015; Lisi and Morimoto 2015). In our experiment, participants
616 were required to perform steady-state overground and treadmill walking at the same
617 speed and without any perturbations that would have triggered deliberate stepping
618 adaptations. Hence, different levels of high beta CMC during overground and treadmill
619 walking may reflect differences in gait stability, step adaptations, sensorimotor
620 processing and/or speed control in each gait condition in our study.

621 If the spectral changes reflect an evoked response as suggested above, the time-
622 frequency profile of power and ITC changes may reflect the waveform of the additive
623 response rather than a change in cortical oscillations. High beta ITC of the TA muscle
624 was significantly enhanced during overground compared to treadmill walking, while no
625 differences in cortical ITC was observed. Hence, the observed differences between
626 treadmill and overground walking may reflect a change in the evoked response in the
627 TA muscle. Possibly, changes in the evoked TA response may be related to peripheral
628 mechanisms involved in stride time or cadence, as these parameters were significantly
629 different between treadmill and overground walking in the present study. This
630 interpretation is supported by studies that showed biomechanical differences between
631 overground and treadmill gait (Carpinella et al. 2010; Chiu et al. 2015; Dingwell et al.
632 2001; Lee and Hidler 2008; Ochoa et al. 2017). In line with this, these potential changes
633 in evoked TA responses could be due to differences in background electrical activity of
634 dorsal horn spinal neurons. In cats, for example, it has been shown that amplitude
635 fluctuations of somatosensory evoked field potentials are positively correlated with
636 spontaneous activity of dorsal horn spinal cord neurons (Manjarrez et al. 2002a;
637 Manjarrez et al. 2002b).

638 **Functional implications**

639 We found positive time lags between coherent EEG and EMG activity at alpha,
640 beta and gamma frequencies, which was consistent for overground and treadmill
641 walking. A positive time lag is consistent with efferent descending activity and hence
642 provides further evidence for efferent cortical control during walking in humans (Artoni
643 et al. 2017; Petersen et al. 2012). The estimated time lags varied from approximately 12

644 ms in the lower beta band to 30 ms in the alpha band. The time lag at low beta
645 frequencies (~12 ms) is consistent with previous studies investigating beta-band CMC
646 in upper limb muscles during isometric contractions, e.g. 11 ms (Mehrkanoon et al.
647 2014), 15.9 ms (Mima et al. 2000), 9.3 ms (Gerloff et al. 2006) and 7.9 ms (Witham et
648 al. 2011). However, this time lag is shorter than the corticospinal conduction time from
649 the cortex to the TA measured by stimulation (roughly 27 ms, Gross et al. 2000;
650 Petersen et al. 2001; Rothwell et al. 1991; Schubert et al. 1997). Indeed, the time delay
651 estimated from phase spectra appears to underestimate the actual physiological
652 corticospinal conduction times (Witham et al. 2011). Hence, while the absolute time lag
653 found in the current study may be an underestimation of the actual conduction time, a
654 positive time lag was robust at the group level and consistent with a cortical drive to the
655 TA muscle during overground and treadmill walking. Although the time lag from cortex
656 to muscle may be consistent with efferent activity, the temporal precedence does not
657 demonstrate that CMC was generated by the influence that the cortex exerts over the
658 spinal motor pool. That is, interpretations in terms of effective connectivity require an
659 explicit model of that influence (Friston 2011).

660 By estimating the time lag of coherent activity, the approach assesses the temporal
661 precedence between signals similar to other methods of directed functional connectivity
662 (Friston et al. 2013). It rests on the assumption that dependencies reflect an underlying
663 dynamical process, in which causes precede consequences. That is, neuronal
664 interactions are based on synaptic connections and hence involve propagation delays.
665 However, temporal precedence does not necessarily imply a causal influence between
666 the two evaluated channels (Kaminski et al. 2001; Seth 2010). It is possible that the
667 effect is mediated by another channel or by another group of channels, or by variables

668 that are not included in the measurements. This caveat is particularly relevant in the
669 current study, in which the results of time-frequency results are consistent with an
670 evoked response. It is likely that the cortical and spinal input underlying the evoked
671 responses are partly generated by other neural systems that were not measured in the
672 current study. The interpretation of the observed time lag in terms of efferent and
673 afferent processes should hence be made with caution.

674 **Limitations**

675 Ambulatory EEG is susceptible to movement artefacts and caution should hence
676 be exerted when interpreting phasic changes in EEG activity (Castermans et al. 2014;
677 Costa et al. 2016; Gwin et al. 2010; Kline et al. 2015; Nathan and Contreras-Vidal
678 2016; Oliveira et al. 2016; Snyder et al. 2015). In this study, we applied multiple
679 strategies to mitigate the effects of motion artefacts: We excluded gait cycles with
680 excessive artefacts, we performed ICA, and we calculated a bipolar derivative EEG
681 signal, which removes further shared artefactual activity across channels similar to a re-
682 referencing approach (Snyder et al. 2015). This way, a bipolar EEG signal reflects
683 nearby cortical activity that is locally generated between the electrode pairs. With
684 respect to the EMG recordings, we high-pass filtered, rectified, and demodulated the
685 signals in order to remove low-frequency artefacts and periodic amplitude modulations
686 that could distort the coherence estimates.

687 The parallel increase in power, ITC and CMC is consistent with an evoked
688 response and it is hence possible that these responses are generated by mechanical
689 artefacts. However, the positive time lags in the alpha, beta and gamma bands suggest
690 that the results of this study were not due to conduction of non-physiological artefacts,

691 which would have likely resulted in a zero time lag (Petersen et al. 2012), but reflect
692 genuine neural activity. The time lag between coherent theta activity was not
693 significantly different from zero, which may suggest residual artefact contamination at
694 theta frequencies specifically. Previous studies indeed found that oscillatory activity at
695 low frequencies may be more affected by movement artefacts than at other/higher
696 frequency ranges (Castermans et al. 2014). The event-related power profiles observed in
697 this study are similar to those in multiple previous studies on cortical oscillatory activity
698 during walking (Artoni et al. 2017; Bradford et al. 2016; Bruijn et al. 2015; Bulea et al.
699 2015; Cheron et al. 2012; Gwin et al. 2011; Knaepen et al. 2015; Severens et al. 2012).
700 This would imply that the observed time-frequency modulations of cortical power and
701 CMC in the current and previous studies reflect genuine neural interactions, or
702 alternatively, are all affected in similar way by non-physiological artefacts. EEG
703 acquisition during dynamic movement remains challenging and methods to minimize
704 movement artefacts in ambulatory EEG is an ongoing pursuit (Kline et al. 2015;
705 Oliveira et al. 2017a; Snyder et al. 2015).

706 **Conclusion**

707 This study shows coherent corticospinal activity during the double support phase
708 of the gait cycle during steady-state overground and treadmill walking in healthy, young
709 adults. Parallel increases in power and ITC suggest evoked responses at spinal and
710 cortical populations rather than a modulation of ongoing corticospinal interactions. A
711 positive time lag between EEG and EMG signals at alpha, beta and gamma frequencies
712 is consistent with efferent activity, but needs to be interpreted with caution. Moreover,
713 this study shows that high beta CMC and ITC of EMG differed between overground

714 and treadmill walking. This may reflect a change in the evoked response in the TA
715 muscle dependent on the gait modality, possibly indicating different peripheral
716 mechanisms that control stride timing. These findings may help to identify
717 neurophysiological mechanisms that are important for understanding cortical control of
718 human gait in health and disease.

719

720 **Appendix**

721 Figure 7 shows EMG data of the right TA of one participant during overground
722 walking. These single participant data are similar to the group average data presented in
723 Figure 1A and B.

724

725

726 **Acknowledgements**

727 We thank Bridie O'Connell and Kathryn McIntosh for support with data collection;
728 Kevin McGill, Steve Mehrkanoon and Christopher Thompson for valuable discussions
729 on the z-transformation of coherence; the QUT HPC and Research Support Group for
730 access to computational resources.

731 **Grants**

732 This work was supported by a Parkinson's Queensland Incorporated PhD project grant.

733 References

734

- 735 **Alton F, Baldey L, Caplan S, and Morrissey MC.** A kinematic comparison of overground and
736 treadmill walking. *Clinical biomechanics (Bristol, Avon)* 13: 434-440, 1998.
- 737 **Amjad AM, Halliday DM, Rosenberg JR, and Conway BA.** An extended difference of coherence
738 test for comparing and combining several independent coherence estimates: Theory and
739 application to the study of motor units and physiological tremor. *J Neurosci Methods* 73: 69-
740 79, 1997.
- 741 **Armstrong DM.** The supraspinal control of mammalian locomotion. *J Physiol* 405: 1-37, 1988.
- 742 **Arsenault AB, Winter DA, and Marteniuk RG.** Treadmill versus walkway locomotion in
743 humans: an EMG study. *Ergonomics* 29: 665-676, 1986.
- 744 **Artoni F, Fanciullacci C, Bertolucci F, Panarese A, Makeig S, Micera S, and Chisari C.**
745 Unidirectional brain to muscle connectivity reveals motor cortex control of leg muscles during
746 stereotyped walking. *NeuroImage* 2017.
- 747 **Boonstra TW, and Breakspear M.** Neural mechanisms of intermuscular coherence:
748 Implications for the rectification of surface electromyography. *J Neurophysiol* 107: 796-807,
749 2012.
- 750 **Boonstra TW, Daffertshofer A, Breakspear M, and Beek PJ.** Multivariate time-frequency
751 analysis of electromagnetic brain activity during bimanual motor learning. *NeuroImage* 36:
752 370-377, 2007.
- 753 **Boonstra TW, Daffertshofer A, Peper CE, and Beek PJ.** Amplitude and phase dynamics
754 associated with acoustically paced finger tapping. *Brain Res* 1109: 60-69, 2006.
- 755 **Boonstra TW, Daffertshofer A, Roerdink M, Flipse I, Groenewoud K, and Beek PJ.** Bilateral
756 motor unit synchronization of leg muscles during a simple dynamic balance task. *Eur J Neurosci*
757 29: 613-622, 2009.
- 758 **Bradford JC, Lukos JR, and Ferris DP.** Electrocortical activity distinguishes between uphill and
759 level walking in humans. *J Neurophysiol* 115: 958-966, 2016.
- 760 **Brantley JA, Luu TP, Ozdemir R, Zhu F, Winslow AT, Huang H, and Contreras-Vidal JL.**
761 Noninvasive EEG correlates of overground and stair walking. *Conf Proc IEEE Eng Med Biol Soc*
762 2016: 5729-5732, 2016.
- 763 **Brujin SM, Van Dieen JH, and Daffertshofer A.** Beta activity in the premotor cortex is
764 increased during stabilized as compared to normal walking. *Frontiers in human neuroscience* 9:
765 593, 2015.
- 766 **Bulea TC, Kim J, Damiano DL, Stanley CJ, and Park HS.** Prefrontal, posterior parietal and
767 sensorimotor network activity underlying speed control during walking. *Frontiers in human*
768 *neuroscience* 9: 247, 2015.
- 769 **Burridge JH, Wood DE, Taylor PN, and McLellan DL.** Indices to describe different muscle
770 activation patterns, identified during treadmill walking, in people with spastic drop-foot. *Med*
771 *Eng Phys* 23: 427-434, 2001.
- 772 **Campanini I, Merlo A, Degola P, Merletti R, Vezzosi G, and Farina D.** Effect of electrode
773 location on EMG signal envelope in leg muscles during gait. *J Electromyogr Kinesiol* 17: 515-
774 526, 2007.

775 **Carpinella I, Crenna P, Rabuffetti M, and Ferrarin M.** Coordination between upper- and lower-
776 limb movements is different during overground and treadmill walking. *Eur J Appl Physiol* 108:
777 71-82, 2010.

778 **Castermans T, and Duvinage M.** Corticomuscular coherence revealed during treadmill walking:
779 further evidence of supraspinal control in human locomotion. *J Physiol* 591: 1407-1408, 2013.

780 **Castermans T, Duvinage M, Cheron G, and Dutoit T.** About the cortical origin of the low-delta
781 and high-gamma rhythms observed in EEG signals during treadmill walking. *Neurosci Lett* 561:
782 166-170, 2014.

783 **Cheron G, Duvinage M, De Saedeleer C, Castermans T, Bengoetxea A, Petieau M,
784 Seetharaman K, Hoellinger T, Dan B, Dutoit T, Sylos Labini F, Lacquaniti F, and Ivanenko Y.**
785 From spinal central pattern generators to cortical network: Integrated BCI for walking
786 rehabilitation. *Neural Plast* 2012: 375148, 2012.

787 **Chiu SL, Chang CC, and Chou LS.** Inter-joint coordination of overground versus treadmill
788 walking in young adults. *Gait Posture* 41: 316-318, 2015.

789 **Conway BA, Halliday DM, Farmer SF, Shahani U, Maas P, Weir AI, and Rosenberg JR.**
790 Synchronization between motor cortex and spinal motoneuronal pool during the performance
791 of a maintained motor task in man. *J Physiol* 489: 917-924, 1995.

792 **Costa A, Salazar-Varas R, Ubeda A, and Azorin JM.** Characterization of artifacts produced by
793 gel displacement on non-invasive brain-machine interfaces during ambulation. *Front Neurosci*
794 10: 60, 2016.

795 **Courtine G, and Schieppati M.** Human walking along a curved path. II. Gait features and EMG
796 patterns. *Eur J Neurosci* 18: 191-205, 2003.

797 **Delorme A, and Makeig S.** EEGLAB Wikitorial
798 [https://sccn.ucsd.edu/wiki/EEGLAB#The EEGLAB Tutorial Outline](https://sccn.ucsd.edu/wiki/EEGLAB#The_EEGLAB_Tutorial_Outline). [accessed in March 2017].

799 **Delorme A, and Makeig S.** EEGLAB: an open source toolbox for analysis of single-trial EEG
800 dynamics including independent component analysis. *J Neurosci Methods* 134: 9-21, 2004.

801 **den Otter AR, Geurts AC, Mulder T, and Duysens J.** Speed related changes in muscle activity
802 from normal to very slow walking speeds. *Gait Posture* 19: 270-278, 2004.

803 **Dingwell JB, Cusumano JP, Cavanagh PR, and Sternad D.** Local dynamic stability versus
804 kinematic variability of continuous overground and treadmill walking. *J Biomech Eng* 123: 27-
805 32, 2001.

806 **Drew T, Andujar J-E, Lajoie K, and Yakovenko S.** Cortical mechanisms involved in visuomotor
807 coordination during precision walking. *Brain Res Rev* 57: 199-211, 2008.

808 **Farina D, Negro F, and Jiang N.** Identification of common synaptic inputs to motor neurons
809 from the rectified electromyogram. *J Physiol* 591: 2403-2418, 2013.

810 **Fell J, Dietl T, Grunwald T, Kurthen M, Klaver P, Trautner P, Schaller C, Elger CE, and
811 Fernandez G.** Neural bases of cognitive ERPs: more than phase reset. *Journal of cognitive
812 neuroscience* 16: 1595-1604, 2004.

813 **Friston K, Moran R, and Seth AK.** Analysing connectivity with Granger causality and dynamic
814 causal modelling. *Current opinion in neurobiology* 23: 172-178, 2013.

815 **Friston KJ.** Functional and effective connectivity: a review. *Brain connectivity* 1: 13-36, 2011.

816 **Fukuyama H, Ouchi Y, Matsuzaki S, Nagahama Y, Yamauchi H, Ogawa M, Kimura J, and
817 Shibasaki H.** Brain functional activity during gait in normal subjects: A SPECT study. *Neurosci
818 Lett* 228: 183-186, 1997.

819 **Gerloff C, Braun C, Staudt M, Hegner YL, Dichgans J, and Krageloh-Mann I.** Coherent
820 corticomuscular oscillations originate from primary motor cortex: Evidence from patients with
821 early brain lesions. *Hum Brain Mapp* 27: 789-798, 2006.

822 **Grillner S.** Neurobiological bases of rhythmic motor acts in vertebrates. *Science* 228: 143-149,
823 1985.

824 **Gross J, Tass PA, Salenius S, Hari R, Freund HJ, and Schnitzler A.** Cortico-muscular
825 synchronization during isometric muscle contraction in humans as revealed by
826 magnetoencephalography. *J Physiol* 527: 623-631, 2000.

827 **Gwin JT, Gramann K, Makeig S, and Ferris DP.** Electro cortical activity is coupled to gait cycle
828 phase during treadmill walking. *NeuroImage* 54: 1289-1296, 2011.

829 **Gwin JT, Gramann K, Makeig S, and Ferris DP.** Removal of movement artifact from high-
830 density EEG recorded during walking and running. *J Neurophysiol* 103: 3526-3534, 2010.

831 **Halliday DM, Conway BA, Christensen LOD, Hansen NL, Petersen NP, and Nielsen JB.**
832 Functional coupling of motor units is modulated during walking in human subjects. *J*
833 *Neurophysiol* 89: 960-968, 2003.

834 **Halliday DM, and Farmer SF.** On the need for rectification of surface EMG. *J Neurophysiol* 103:
835 3547, 2010.

836 **Halliday DM, Rosenberg JR, Amjad AM, Breeze P, Conway BA, and Farmer SF.** A framework
837 for the analysis of mixed time series/point process data—Theory and application to the study
838 of physiological tremor, single motor unit discharges and electromyograms. *Progress in*
839 *biophysics and molecular biology* 64: 237-278, 1995.

840 **Kaminski M, Ding M, Truccolo WA, and Bressler SL.** Evaluating causal relations in neural
841 systems: granger causality, directed transfer function and statistical assessment of significance.
842 *Biol Cybern* 85: 145-157, 2001.

843 **Kline JE, Huang HJ, Snyder KL, and Ferris DP.** Cortical Spectral Activity and Connectivity during
844 Active and Viewed Arm and Leg Movement. *Front Neurosci* 10: 91, 2016.

845 **Kline JE, Huang HJ, Snyder KL, and Ferris DP.** Isolating gait-related movement artifacts in
846 electroencephalography during human walking. *Journal of neural engineering* 12: 046022,
847 2015.

848 **Knaepen K, Mierau A, Swinnen E, Tellez HF, Michielsen M, Kerckhofs E, Lefeber D, and**
849 **Meeusen R.** Human-robot interaction: Does robotic guidance force affect gait-related brain
850 dynamics during robot-assisted treadmill walking? *PLoS ONE* 10: e0140626, 2015.

851 **la Fougère C, Zwergal A, Rominger A, Förster S, Fesl G, Dieterich M, Brandt T, Strupp M,**
852 **Bartenstein P, and Jahn K.** Real versus imagined locomotion: A [18F]-FDG PET-fMRI
853 comparison. *NeuroImage* 50: 1589-1598, 2010.

854 **Lee SJ, and Hidler J.** Biomechanics of overground vs. treadmill walking in healthy individuals.
855 *Journal of applied physiology (Bethesda, Md : 1985)* 104: 747-755, 2008.

856 **Lisi G, and Morimoto J.** EEG single-trial detection of gait speed changes during treadmill walk.
857 *PLoS ONE* 10: e0125479, 2015.

858 **Long J, Tazoe T, Soteropoulos DS, and Perez MA.** Interhemispheric connectivity during
859 bimanual isometric force generation. *J Neurophysiol* 115: 1196-1207, 2015.

860 **Luu TP, Brantley JA, Nakagome S, Zhu F, and Contreras-Vidal JL.** Electro cortical correlates of
861 human level-ground, slope, and stair walking. *PLoS ONE* 12: e0188500, 2017.

862 **Makeig S, Debener S, Onton J, and Delorme A.** Mining event-related brain dynamics. *Trends in*
863 *cognitive sciences* 8: 204-210, 2004.

864 **Manjarrez E, Rojas-Piloni G, Martinez L, Vazquez D, Velez D, Mendez I, and Flores A.**
865 Amplitude of somatosensory cortical evoked potentials is correlated with spontaneous activity
866 of spinal neurones in the cat. *Neurosci Lett* 323: 187-190, 2002a.

867 **Manjarrez E, Rojas-Piloni G, Vazquez D, and Flores A.** Cortical neuronal ensembles driven by
868 dorsal horn spinal neurones with spontaneous activity in the cat. *Neurosci Lett* 318: 145-148,
869 2002b.

870 **Mazaheri A, and Jensen O.** Rhythmic pulsing: linking ongoing brain activity with evoked
871 responses. *Frontiers in human neuroscience* 4: 177, 2010.

872 **McClelland VM, Cvetkovic Z, and Mills KR.** Rectification of the EMG is an unnecessary and
873 inappropriate step in the calculation of Corticomuscular coherence. *J Neurosci Methods* 205:
874 190-201, 2012.

875 **Mehrkanoon S, Breakspear M, and Boonstra TW.** The reorganization of corticomuscular
876 coherence during a transition between sensorimotor states. *NeuroImage* 100: 692-702, 2014.

877 **Mima T, and Hallett M.** Electroencephalographic analysis of cortico-muscular coherence:
878 Reference effect, volume conduction and generator mechanism. *Clinical neurophysiology :
879 official journal of the International Federation of Clinical Neurophysiology* 110: 1892-1899,
880 1999.

881 **Mima T, Steger J, Schulman AE, Gerloff C, and Hallett M.** Electroencephalographic
882 measurement of motor cortex control of muscle activity in humans. *Clinical neurophysiology :
883 official journal of the International Federation of Clinical Neurophysiology* 111: 326-337, 2000.

884 **Miyai I, Tanabe HC, Sase I, Eda H, Oda I, Konishi I, Tsunazawa Y, Suzuki T, Yanagida T, and
885 Kubota K.** Cortical mapping of gait in humans: A near-infrared spectroscopic topography study.
886 *NeuroImage* 14: 1186-1192, 2001.

887 **Nathan K, and Contreras-Vidal JL.** Negligible motion artifacts in scalp electroencephalography
888 (EEG) during treadmill walking. *Frontiers in human neuroscience* 9: 708, 2016.

889 **Neto OP, and Christou EA.** Rectification of the EMG signal impairs the identification of
890 oscillatory input to the muscle. *J Neurophysiol* 103: 1093-1103, 2010.

891 **Ochoa J, Sternad D, and Hogan N.** Treadmill versus Overground Walking: Different Response
892 to Physical Interaction. *J Neurophysiol* jn.00176.02017, 2017.

893 **Oliveira AS, Schlink BR, Hairston WD, Konig P, and Ferris DP.** A Channel Rejection Method for
894 Attenuating Motion-Related Artifacts in EEG Recordings during Walking. *Front Neurosci* 11:
895 225, 2017a.

896 **Oliveira AS, Schlink BR, Hairston WD, Konig P, and Ferris DP.** Induction and separation of
897 motion artifacts in EEG data using a mobile phantom head device. *Journal of neural
898 engineering* 13: 036014, 2016.

899 **Oliveira AS, Schlink BR, Hairston WD, Konig P, and Ferris DP.** Restricted vision increases
900 sensorimotor cortex involvement in human walking. *J Neurophysiol* jn.00926.02016, 2017b.

901 **Perry J.** *Gait analysis: normal and pathological function.* Thorofare, N.J: SLACK, 1992.

902 **Petersen NT, Butler JE, Marchand-Pauvert V, Fisher R, Ledebt A, Pyndt HS, Hansen NL, and
903 Nielsen JB.** Suppression of EMG activity by transcranial magnetic stimulation in human
904 subjects during walking. *J Physiol* 537: 651-656, 2001.

905 **Petersen TH, Willerslev-Olsen M, Conway BA, and Nielsen JB.** The motor cortex drives the
906 muscles during walking in human subjects. *J Physiol* 590: 2443-2452, 2012.

907 **Pfurtscheller G, and Lopes da Silva FH.** Event-related EEG/MEG synchronization and
908 desynchronization: Basic principles. *Clinical neurophysiology : official journal of the
909 International Federation of Clinical Neurophysiology* 110: 1842-1857, 1999.

910 **Pikovsky A, Rosenblum M, and Kurths J.** *Synchronization: a universal concept in nonlinear
911 sciences.* Cambridge University Press, 2003.

912 **Raethjen J, Lindemann M, Dimpelmann M, Wenzelburger R, Stolze H, Pfister G, Elger CE,
913 Timmer J, and Deuschl G.** Corticomuscular coherence in the 6-15 Hz band: is the cortex
914 involved in the generation of physiologic tremor? *Experimental brain research Experimentelle
915 Hirnforschung Experimentation cerebrale* 142: 32-40, 2002.

916 **Riley PO, Paolini G, Della Croce U, Paylo KW, and Kerrigan DC.** A kinematic and kinetic
917 comparison of overground and treadmill walking in healthy subjects. *Gait Posture* 26: 17-24,
918 2007.

919 **Ritter P, and Becker R.** Detecting alpha rhythm phase reset by phase sorting: caveats to
920 consider. *NeuroImage* 47: 1-4, 2009.

921 **Rothwell JC, Thompson PD, Day BL, Boyd S, and Marsden CD.** Stimulation of the human
922 motor cortex through the scalp. *Exp Physiol* 76: 159-200, 1991.

923 **Schubert M, Curt A, Jensen L, and Dietz V.** Corticospinal input in human gait: Modulation of
924 magnetically evoked motor responses. *Experimental brain research Experimentelle
925 Hirnforschung Experimentation cerebrale* 115: 234-246, 1997.

926 **Seeber M, Scherer R, Wagner J, Solis-Escalante T, and Muller-Putz GR.** EEG beta suppression
927 and low gamma modulation are different elements of human upright walking. *Frontiers in
928 human neuroscience* 8: 485, 2014.

929 **Seeber M, Scherer R, Wagner J, Solis-Escalante T, and Müller-Putz GR.** High and low gamma
930 EEG oscillations in central sensorimotor areas are conversely modulated during the human gait
931 cycle. *NeuroImage* 112: 318-326, 2015.

932 **Seth AK.** A MATLAB toolbox for Granger causal connectivity analysis. *J Neurosci Methods* 186:
933 262-273, 2010.

934 **Severens M, Nienhuis B, Desain P, and Duysens J.** Feasibility of measuring event related
935 desynchronization with electroencephalography during walking. *Conf Proc IEEE Eng Med Biol
936 Soc* 2012: 2764-2767, 2012.

937 **Shah AS, Bressler SL, Knuth KH, Ding M, Mehta AD, Ulbert I, and Schroeder CE.** Neural
938 dynamics and the fundamental mechanisms of event-related brain potentials. *Cerebral cortex
939 (New York, NY : 1991)* 14: 476-483, 2004.

940 **Sipp AR, Gwin JT, Makeig S, and Ferris DP.** Loss of balance during balance beam walking elicits
941 a multifocal theta band electrocortical response. *J Neurophysiol* 110: 2050-2060, 2013.

942 **Snyder KL, Kline JE, Huang HJ, and Ferris DP.** Independent Component Analysis of gait-related
943 movement artifact recorded using EEG electrodes during treadmill walking. *Frontiers in human
944 neuroscience* 9: 639, 2015.

945 **Storzer L, Butz M, Hirschmann J, Abbasi O, Gratkowski M, Saupe D, Schnitzler A, and Dalal SS.**
946 Bicycling and walking are associated with different cortical oscillatory dynamics. *Frontiers in
947 human neuroscience* 10: 61, 2016.

948 **Sutherland DH.** The evolution of clinical gait analysis part I: kinesiological EMG. *Gait Posture*
949 14: 61-70, 2001.

950 **Tallon-Baudry C, Bertrand O, Delpuech C, and Pernier J.** Stimulus specificity of phase-locked
951 and non-phase-locked 40 Hz visual responses in human. *The Journal of neuroscience : the
952 official journal of the Society for Neuroscience* 16: 4240-4249, 1996.

953 **Wagner J, Makeig S, Gola M, Neuper C, and Muller-Putz G.** Distinct beta band oscillatory
954 networks subserving motor and cognitive control during gait adaptation. *The Journal of
955 neuroscience : the official journal of the Society for Neuroscience* 36: 2212-2226, 2016.

956 **Wagner J, Solis-Escalante T, Grieshofer P, Neuper C, Muller-Putz G, and Scherer R.** Level of
957 participation in robotic-assisted treadmill walking modulates midline sensorimotor EEG
958 rhythms in able-bodied subjects. *NeuroImage* 63: 1203-1211, 2012.

959 **Wagner J, Solis-Escalante T, Scherer R, Neuper C, and Muller-Putz G.** It's how you get there:
960 Walking down a virtual alley activates premotor and parietal areas. *Frontiers in human
961 neuroscience* 8: 93, 2014.

962 **Ward NJ, Farmer SF, Berthouze L, and Halliday DM.** Rectification of EMG in low force
963 contractions improves detection of motor unit coherence in the beta-frequency band. *J
964 Neurophysiol* 110: 1744-1750, 2013.

965 **White SC, Yack HJ, Tucker CA, and Lin HY.** Comparison of vertical ground reaction forces
966 during overground and treadmill walking. *Med Sci Sports Exerc* 30: 1537-1542, 1998.

967 **Winslow AT, Brantley J, Zhu F, Contreras Vidal JL, and Huang H.** Corticomuscular coherence
968 variation throughout the gait cycle during overground walking and ramp ascent: A preliminary
969 investigation. *Conf Proc IEEE Eng Med Biol Soc* 2016: 4634-4637, 2016.

970 **Witham CL, Riddle CN, Baker MR, and Baker SN.** Contributions of descending and ascending
971 pathways to corticomuscular coherence in humans. *J Physiol* 589: 3789-3800, 2011.
972 **Yang JF, and Winter DA.** Electromyographic amplitude normalization methods: improving their
973 sensitivity as diagnostic tools in gait analysis. *Arch Phys Med Rehabil* 65: 517-521, 1984.
974 **Yoshida T, Masani K, Zabjek K, Chen R, and Popovic MR.** Dynamic Increase in Corticomuscular
975 Coherence during Bilateral, Cyclical Ankle Movements. *Frontiers in human neuroscience* 11:
976 155, 2017.
977

978

979

980 **Figure Captions**

981 **Figure 1. Grand-average EMG envelopes and time-frequency EEG power spectra.**

982 EMG envelopes of the right (A) and left (B) TA during overground (orange) and
983 treadmill (green) walking. EEG PSD acquired from bipolar EEG signals of the left
984 sensorimotor cortex (C3-F3) during overground (C) and treadmill walking (E), and of
985 the right sensorimotor cortex (C4-F4) during overground (D) and treadmill walking (F),
986 showing the percent change from the average. X-axis shows time points of gait cycle in
987 seconds, relative to heel strike ($t=0$) of the left (B, D, F) and right (A, C, E) foot. LHS,
988 left heel strike; LTO, left toe-off; SMC, sensorimotor cortex; RHS, right heel strike;
989 RTO, right toe-off; TA, tibialis anterior.

990

991 **Figure 2. Grand-average EEG power, CMC and ITC during double support.**

992 Data during double support (0-125 ms) averaged across sides/channels (C3F3, C4F4 for
993 EEG data; TAl and TAr for EMG data), depicted for each frequency band (theta, alpha,
994 low beta, high beta, gamma) during overground and treadmill walking. Bars show the
995 group mean, vertical lines show two SEM (± 1 SEM). Significant differences between
996 overground and treadmill conditions are marked with asterisks. (A) Normalized EEG
997 PSD, (B) z-transformed coherence, (C) EEG inter-trial coherence, (D) EMG inter-trial
998 coherence. CMC, corticomuscular coherence; ITC, inter-trial coherence; TA, tibialis
999 anterior.

1000

1001 **Figure 3. Grand-average time-frequency coherence between EEG and EMG.**

1002 Corticomuscular coherence between bipolar EEG from the left sensorimotor cortex
1003 (C3F3) and EMG from the right TA during overground (A) and treadmill (C) walking;
1004 coherence of bipolar EEG from the right sensorimotor cortex (C4F4) and EMG from the
1005 left TA during overground (B) and treadmill (D) walking. X-axis shows time points of
1006 gait cycle in seconds, relative to heel strike ($t=0$) of the left (B, D) and right (A, C) foot.
1007 Y-axis shows frequencies in Hz. Colour-coding shows the coherence value. LHS, left

1008 heel strike; LTO, left toe-off; SMC, sensorimotor cortex; RHS, right heel strike; RTO,
1009 right toe-off; TA, tibialis anterior.

1010

1011 **Figure 4. Grand-average time-frequency EEG inter-trial coherence.**

1012 Inter-trial coherence of the bipolar EEG signals of the left sensorimotor cortex (C3-F3)
1013 during overground (A) and treadmill walking (C), and of the right sensorimotor cortex
1014 (C4-F4) during overground (B) and treadmill walking (D). X-axis shows time points of
1015 gait cycle in seconds, relative to heel strike ($t=0$) of the left (B, D) and right (A, C) foot.
1016 Non-significant values are masked in black. LHS, left heel strike; LTO, left toe-off;
1017 SMC, sensorimotor cortex; RHS, right heel strike; RTO, right toe-off.

1018

1019 **Figure 5. Grand-average time-frequency TA EMG inter-trial coherence.**

1020 Inter-trial coherence of the EMG signals of the left TA during overground (A) and
1021 treadmill walking (C), and of the right TA during overground (B) and treadmill walking
1022 (D). X-axis shows time points of gait cycle in seconds, relative to heel strike ($t=0$) of the
1023 left (A, C) and right (B, D) foot. Non-significant values are masked in black. LHS, left
1024 heel strike; LTO, left toe-off; RHS, right heel strike; RTO, right toe-off; TA, tibialis
1025 anterior.

1026

1027 **Figure 6. Estimation of time lag between EEG and EMG.**

1028 (A) Corticomuscular coherence between bipolar EEG from the sensorimotor cortex and
1029 contralateral TA EMG at the time point +50 ms (mid double support) during
1030 overground walking. Data were averaged across sides/channels (C3F3-TAr, C4F4-TAl).
1031 Grey patches indicate low beta frequency range (13-21 Hz), dots depict FFT frequency
1032 bins with significant CMC, horizontal dashed line shows upper limit of 95% CI. (B)
1033 Corresponding phase spectrum and fitted regression line in the lower beta band. (C)
1034 Estimated mean time lag between EEG and EMG in each frequency band (averaged
1035 across overground and treadmill, as statistical analyses identified no significant effect of
1036 gait condition on time lag). Bars and dots show the group mean; vertical lines depict the
1037 standard error of the mean. Time lags estimated based on slope of fitted regression line

1038 of individual phase spectra in each frequency band and condition. Positive time lag
1039 values indicate a time lag from EEG to EMG. CI, confidence interval; CMC,
1040 corticomuscular coherence.

1041

1042 **Figure 7. Processing of EMG signals.**

1043 EMG of right TA of one participant during overground walking. (A) Raw EMG (as
1044 recorded) of one step, (B) filtered EMG of one step, (C) filtered and rectified EMG of
1045 one step, (D) Mean of 220 steps (envelope) of filtered and rectified EMG. LHS, left heel
1046 strike; LTO, left toe-off; RHS, right heel strike; RTO, right toe-off; TA, tibialis anterior.

1047

1048

1049 **Tables**

1050

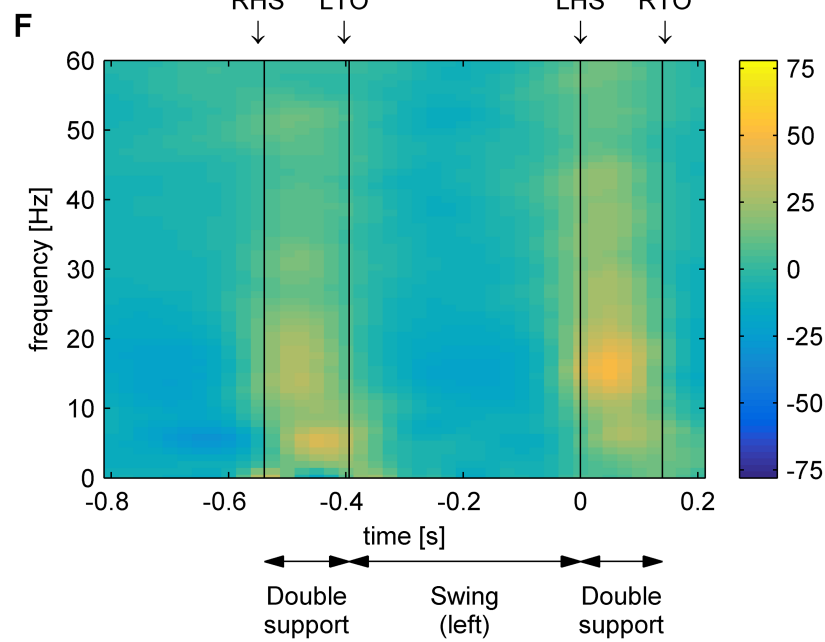
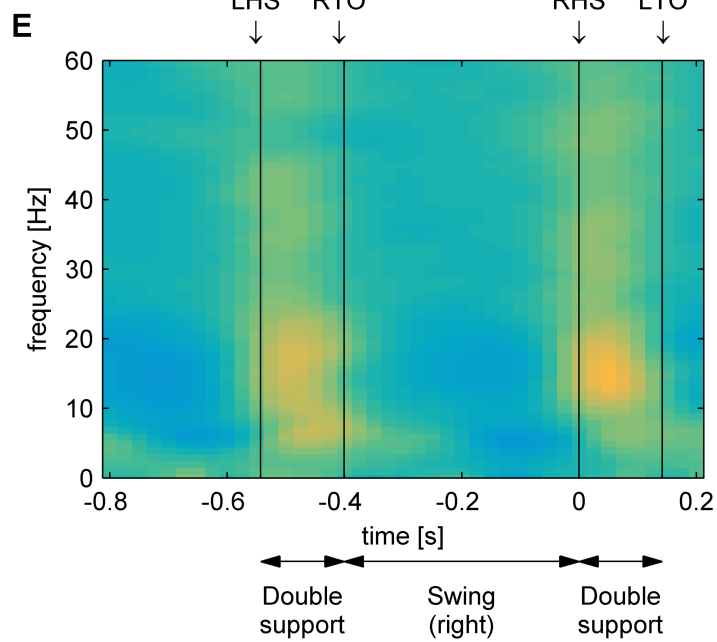
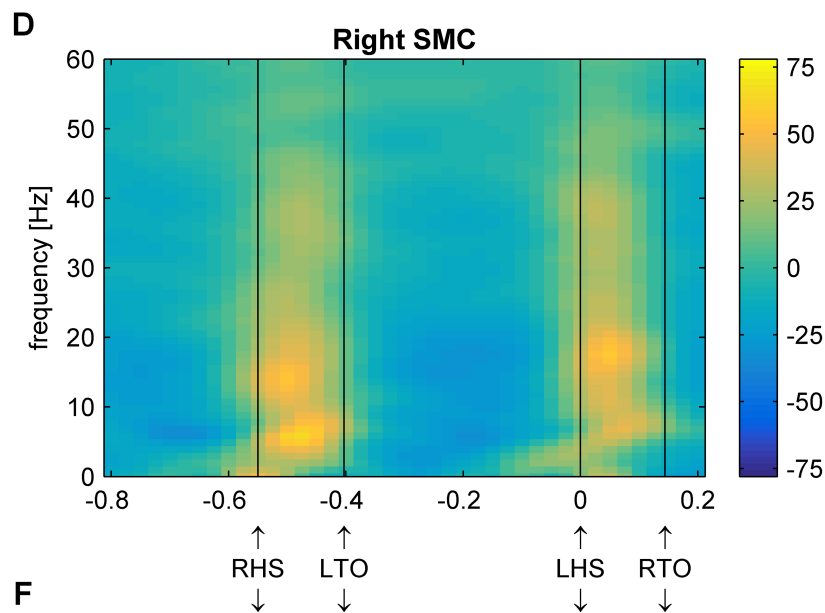
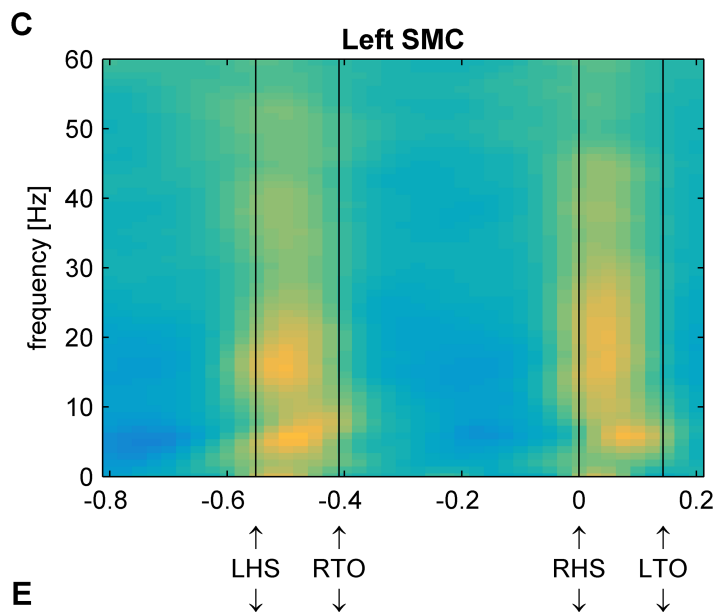
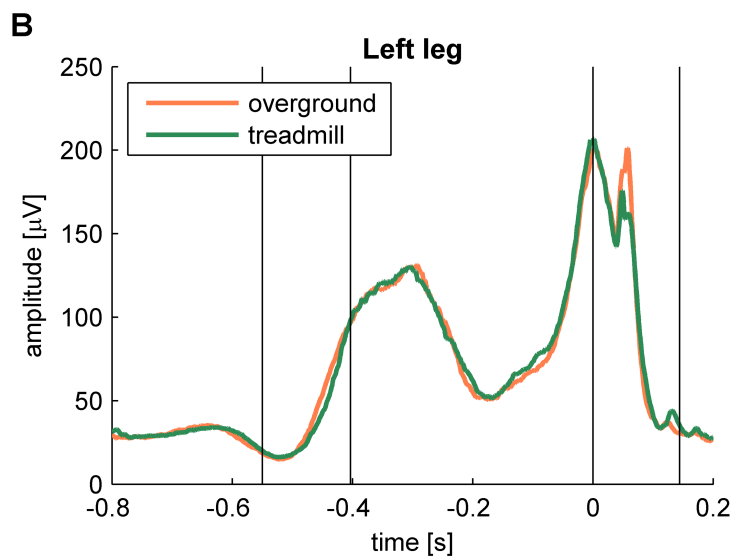
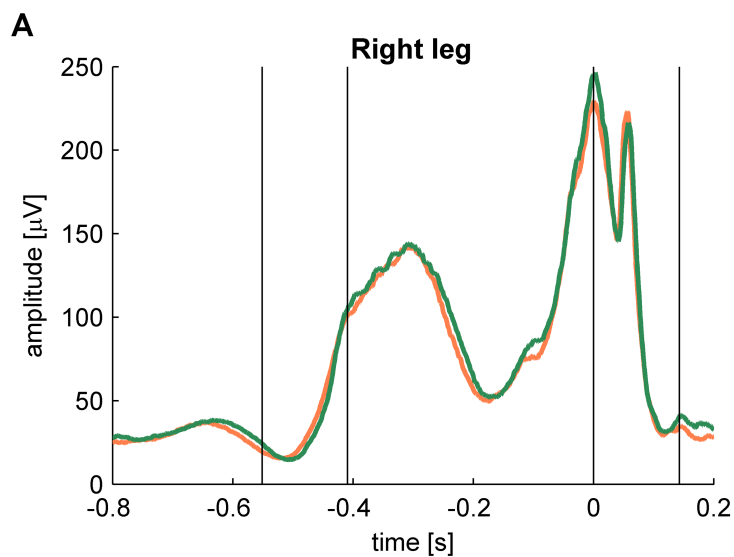
1051 **Table 1. Temporal gait parameters during overground and treadmill walking**

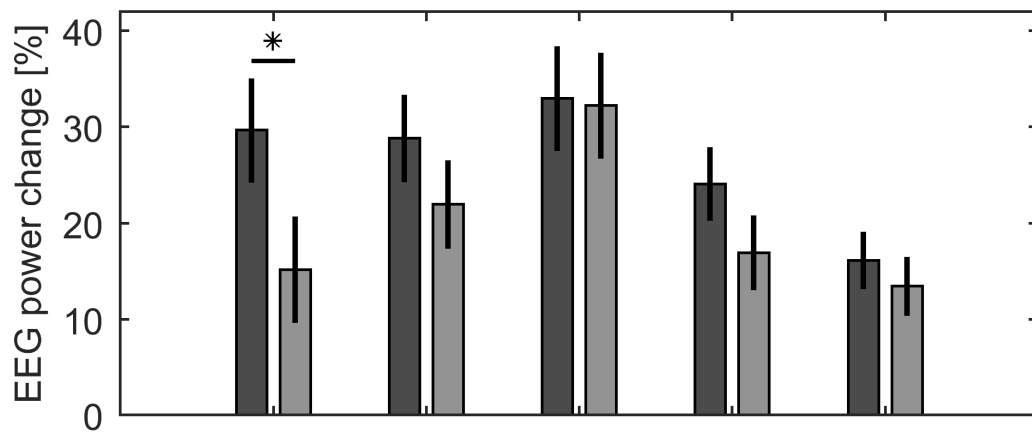
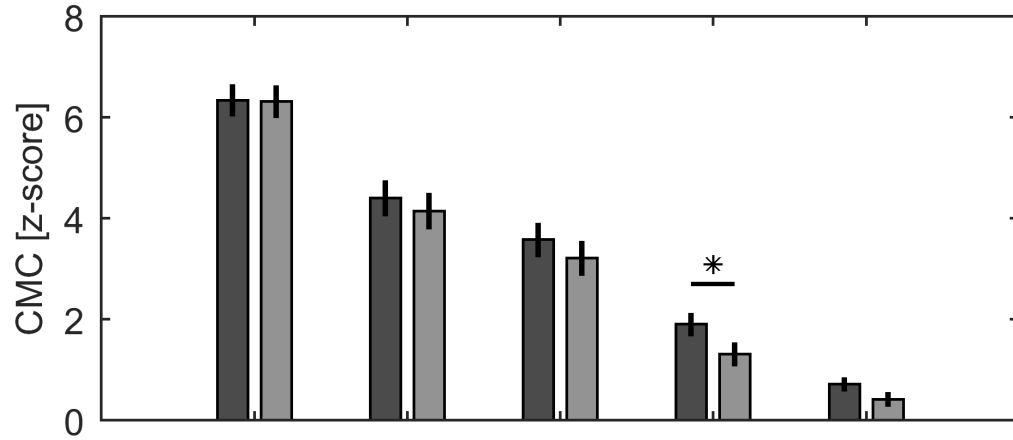
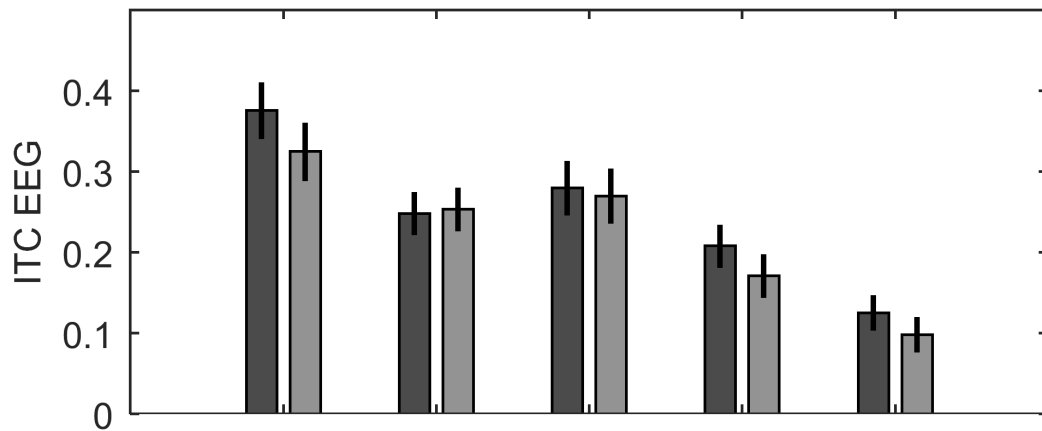
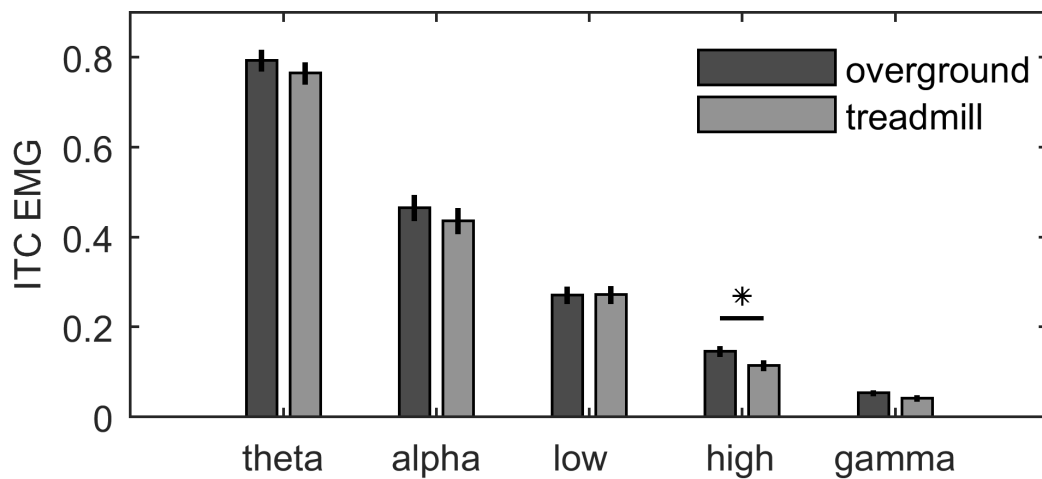
Gait Parameter	Overground mean (SD) n = 22	Treadmill mean (SD) n = 22	T-statistic T(df), p-value
Walking Speed (km h ⁻¹)	4.165 (0.411)*	4.178 (0.421)*	T(18) = -0.934, p = 0.362
Cadence (strides/min)	54.088 (3.817)	55.497 (3.440)	T(21) = -2.750, p = 0.012
Stride time (s)	1.115 (0.080)	1.085 (0.070)	T(21) = 2.998, p = 0.007
Stride time variability (s)	0.020 (0.006)	0.019 (0.019)	T(21) = 0.299, p = 0.768
Step time (s)	0.551 (0.040)	0.544 (0.042)	T(21) = 1.273, p = 0.217
Step time variability (s)	0.011 (0.004)	0.014 (0.021)	T(21) = -0.752, p = 0.460
Stance phase (s)	0.696 (0.072)	0.681 (0.060)	T(21) = 2.043, p = 0.054
Swing phase (s)	0.407 (0.024)	0.401 (0.032)	T(21) = 1.337, p = 0.196
Single support (s)	0.407 (0.024)	0.401 (0.032)	T(21) = 1.337, p = 0.196
Double support (s)	0.144 (0.036)	0.147 (0.046)	T(21) = -0.436, p = 0.667

1052 * n = 19

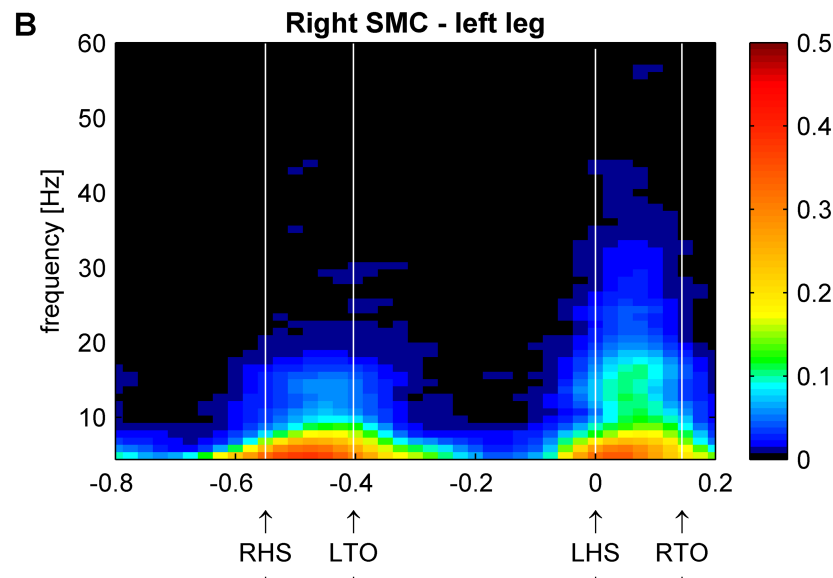
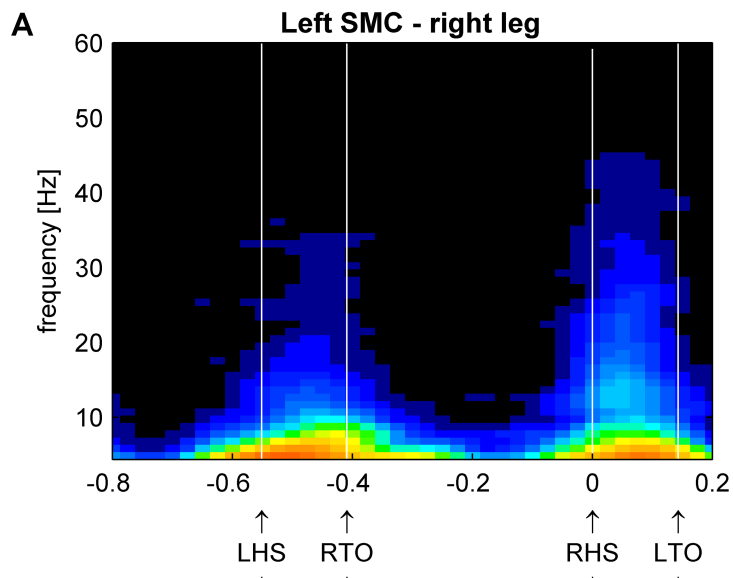
1053

1054

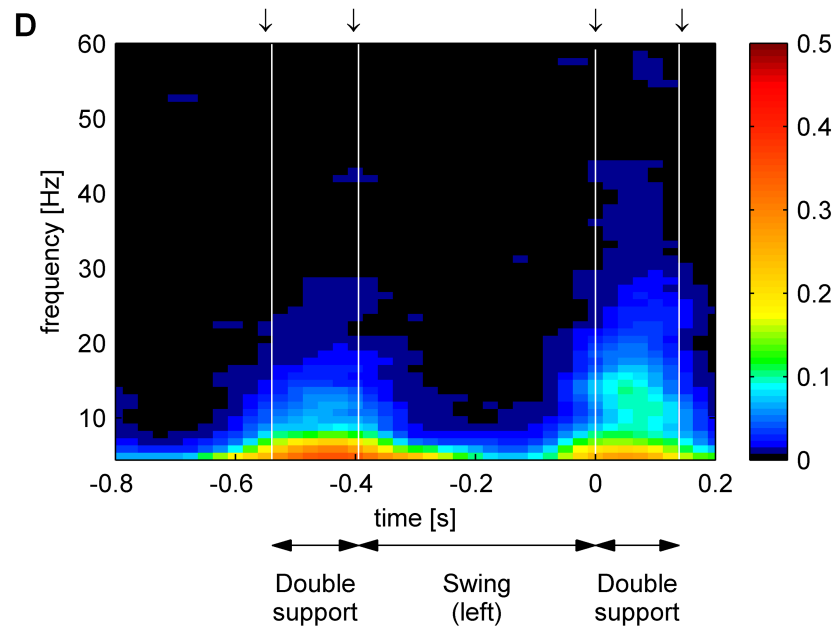
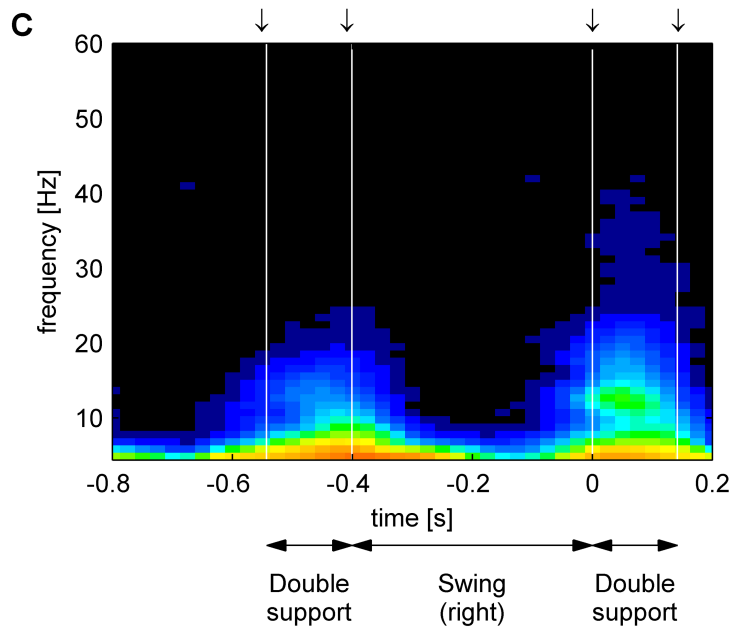


A**B****C****D**

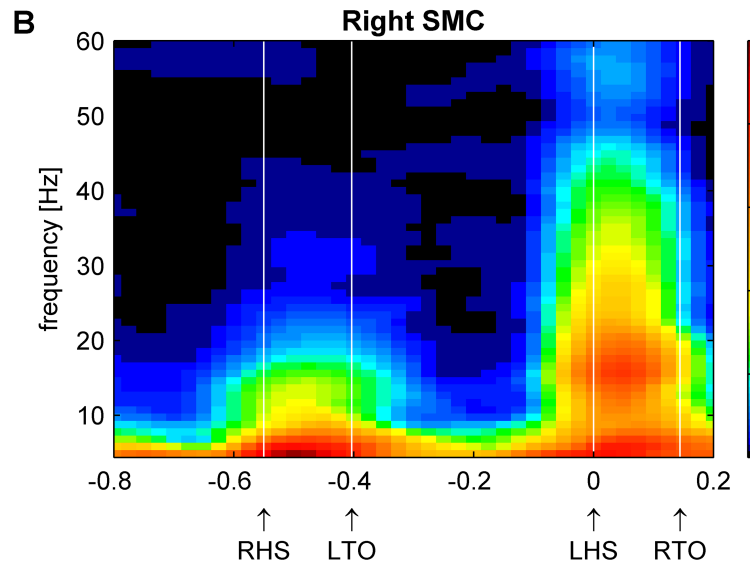
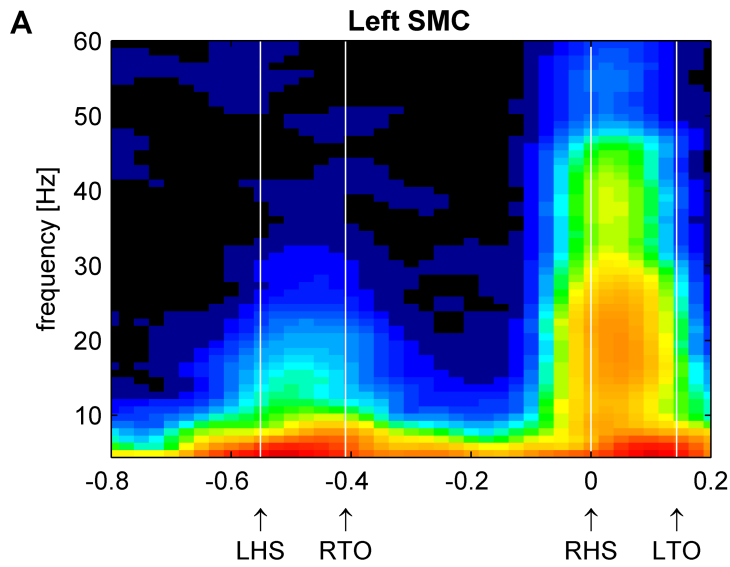
Overground



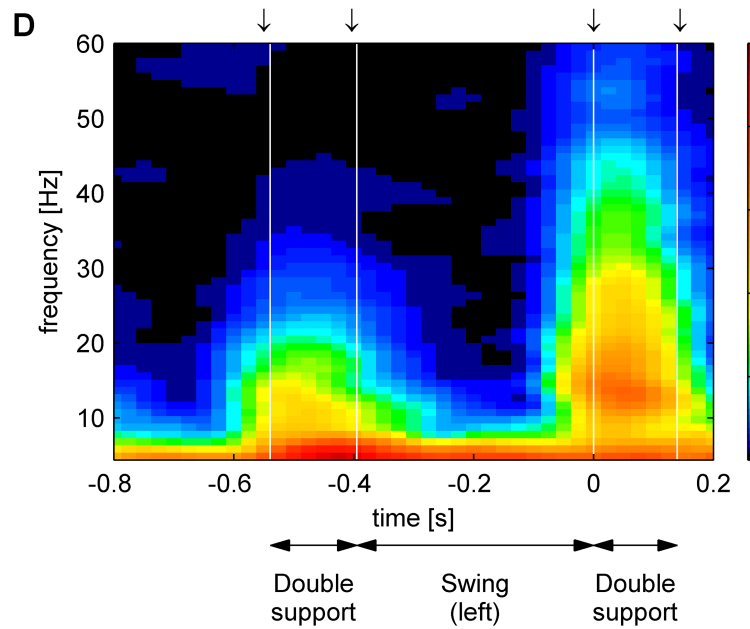
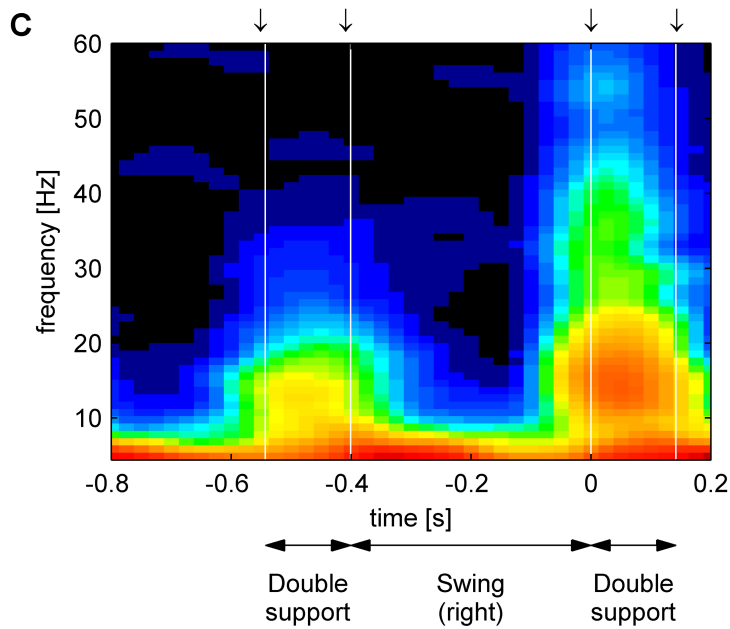
Treadmill



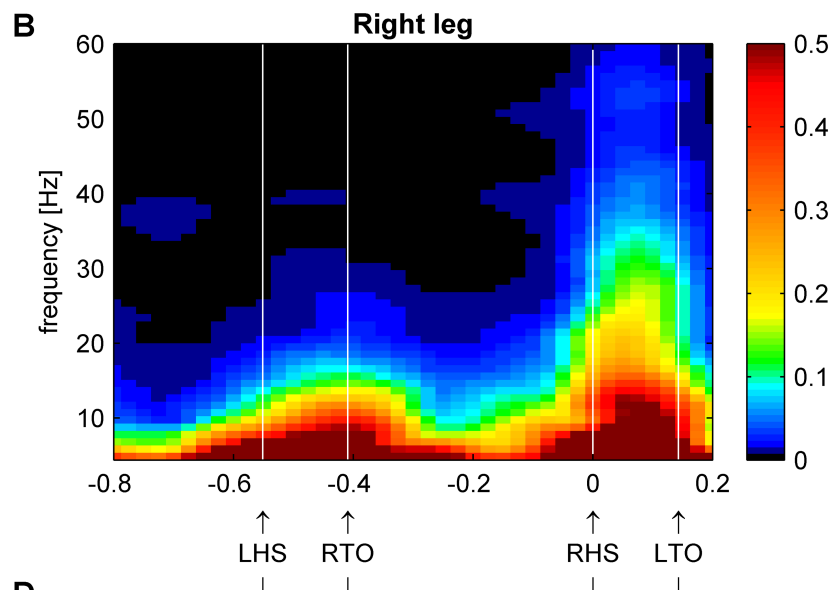
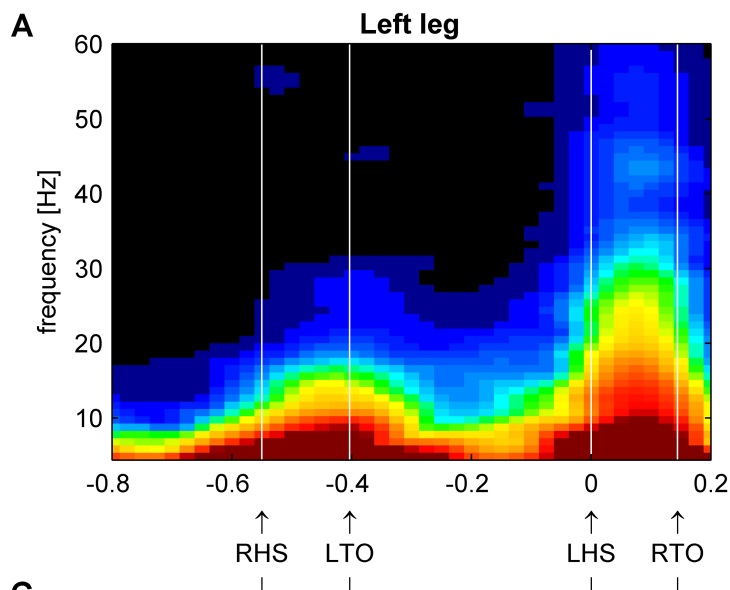
Overground



Treadmill



Overground



Treadmill

